Theoretical analysis of destabilization resonances in time-delayed stochastic second-order dynamical systems and some implications for human motor control.

Patanarapeelert, K.; Frank, T.D.; Friedrich, R.; Beek, P.J.; Tang, I.M.

published in
Physical Review E
2006

DOI (link to publisher)
10.1103/PhysRevE.73.021901

document version
Publisher's PDF, also known as Version of record

Theoretical analysis of destabilization resonances in time-delayed stochastic second-order dynamical systems and some implications for human motor control

K. Patanarapeelert,[1] T. D. Frank,[2] R. Friedrich,[2] P. J. Beek,[3] and I. M. Tang[4]
[1]*Faculty of Science, Department of Mathematics, Mahidol University, Rama VI Road, Bangkok 10400, Thailand*
[2]*Institute for Theoretical Physics, University of Münster, Wilhelm-Klemm-Strasse 9, 48149 Münster, Germany*
[3]*Faculty of Human Movement Sciences, Vrije Universiteit, Van der Boechorststraat 9, 1081 BT Amsterdam, The Netherlands*
[4]*Faculty of Science, Department of Physics, Mahidol University, Rama VI Road, Bangkok 10400, Thailand*
(Received 1 June 2005; revised manuscript received 12 October 2005; published 6 February 2006)

A linear stochastic delay differential equation of second order is studied that can be regarded as a Kramers model with time delay. An analytical expression for the stationary probability density is derived in terms of a Gaussian distribution. In particular, the variance as a function of the time delay is computed analytically for several parameter regimes. Strikingly, in the parameter regime close to the parameter regime in which the deterministic system exhibits Hopf bifurcations, we find that the variance as a function of the time delay exhibits a sequence of pronounced peaks. These peaks are interpreted as delay-induced destabilization resonances arising from oscillatory ghost instabilities. On the basis of the obtained theoretical findings, reinterpretations of previous human motor control studies and predictions for future human motor control studies are provided.

DOI: 10.1103/PhysRevE.73.021901 PACS number(s): 87.19.St, 02.50.Ey, 02.30.Ks, 87.10.+e

I. INTRODUCTION

The effects of time delays on dynamical systems have been studied extensively in recent years. This is appropriate because many complex systems involve feedback of time-delayed system variables. Time-delayed system variables are fed back, for instance, in laser systems with mirrors [1–3], electronic devices [4], chemical surface reactions [5], hydrodynamical phenomena [6], and bistable systems in general [7,8]. Importantly, unstable systems can be controlled and stabilized by means of time-delayed feedback mechanisms [9]. In biology, time delays are frequently used to account for maturation times [10,11], cell division times [12], and signal processing as well as signal transmission times. In the latter context, breathing [13], tracking [14–18], balancing [19–21], postural sway [22–24], isometric force production [25,26], coordinated movement [27], and neural network dynamics [28–33] have been studied (see Ref. [34] for a review). Time delays also occur in the activation of muscles [35] and muscle groups [36].

Most analytical studies on time-delayed systems are concerned with deterministic models [19,37,38]. A common finding in those studies is that the introduction of a time delay into a dynamical system that exhibits a stable fixed point usually results in a destabilization of that fixed point at a critical value of that delay, i.e., in a Hopf bifurcation [37–39]. Deterministic models, however, are unsuitable for modeling complex systems that involve fluctuating sources (or noise sources). Therefore, current research is also dedicated to the analysis of stochastic models with time delays [14,40–48]. In particular, for a linear first-order dynamical system with time delay, the delay-induced Hopf bifurcation has been studied in a stochastic framework [14,40–46,49]. Accordingly, for subcritical delays the system exhibits a stationary Gaussian distribution. At the Hopf bifurcation point, the variance of the Gaussian distribution becomes infinite and the first moment oscillates. That is, the system does not exhibit a stationary distribution any more. Looking at the variance as a function of the time delay, there are three qualitatively different behaviors related to three different parameter regimes, see Fig. 1. First, if the system exhibits a Hopf bifurcation, then the variance increases monotonically as a function of the time delay until it becomes infinite at the Hopf bifurcation point. Second, if the system does not exhibit a Hopf bifurcation, then there are two possibilities: (i) the variance increases to infinity when the time delay is increased such that when the time delay becomes infinitely large the variance becomes infinite, and (ii) the variance increases monotonically and approaches a finite asymptotic value when the time delay becomes infinitely large.

First-order dynamical systems may be interpreted as systems describing overdamped motions. However, there are several systems in which inertia plays an important role and that hence require a description in terms of second-order differential equations with a time delay. Oscillatory systems are a case in point. In this context, the impact of time delays on noise-induced oscillations [50] and the desynchronization of coupled oscillators by means of time-delayed feedback [51] have been discussed. Delay-induced oscillatory modes and

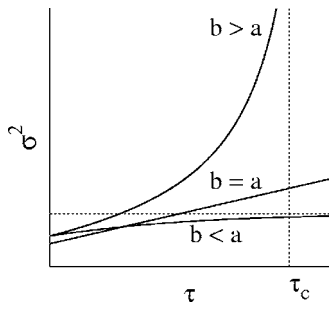

FIG. 1. Qualitative functional dependencies of variances σ_p^2 on time delays τ for first-order dynamical models of the form (5).

limit cycles have also been examined in linear second-order dynamical systems [52,53] and in second-order dynamical systems involving piecewise constant time-delayed feedback [54,55]. In the latter context, chaos has been studied as well [56]. In the study of human motor control, the interplay between inertia and time delays has been studied in the context of balancing [20] and postural control [24]. Furthermore, tracking movements have been studied in terms of second-order dynamical systems for tracking errors [57]. This approach proceeds as follows. If $x_h(t)$ denotes the position of a limb (e.g., arm, hand) tracking a target and $x_t(t)$ denotes the position of the target, then the two-dimensional vector reflecting position and velocity errors is defined by $\mathbf{e}=(x_h-x_t,\dot{x}_h-\dot{x}_t)$. By assuming that the tracking movements are determined by the overall aim to minimize the error $\mathbf{e}$, one may then model the tracking movements directly in terms of an evolution equation for $\mathbf{e}(t)$ rather than an evolution equation for $x_h(t)$. The evolution equation for $\mathbf{e}(t)$ typically reads $\dot{\mathbf{e}}(t)=A\mathbf{e}(t)+B\mathbf{e}(t-\tau)$, where A and B are matrices and τ corresponds to a neurophysiological delay. This error dynamics model is a time-delayed second-order dynamical model when it is written in terms of a single variable $e(t)=x_h(t)-x_t(t)$. Furthermore, we would like to emphasize that man-machine interactions in general, and teleoperating systems in particular, often involve inertia terms [58]. These systems can be conveniently described in terms of master-slave systems, where the human operator corresponds to the master and the machine to the slave. Since the information transfer between master and slave requires finite transmission times, master-slave systems are appropriately modeled as time-delayed dynamical systems. If we think of a simple but nontrivial master-slave system, where the slave responds immediately to the master, then the dynamics is governed by a second-order evolution equation of the form $\ddot{x}(t)=c_1\dot{x}(t)+c_2x(t)+c_3\dot{x}(t-\tau)+c_4x(t-\tau)$, where c_i are parameters, τ corresponds to the transmission delay, and $x(t)$ describes the action of the master. For example, $x(t)$ may describe the position of a moving limb.

As stated in the preceding, for linear first-order dynamical systems involving fluctuating forces and time delays, we have a clear picture about the impact of time delays on system stability and, in particular, we have a good understanding of the stochastic behavior close to the Hopf bifurcation point. The question is how the situation changes when inertia plays a prominent role, as in human motor control systems.

Such time-delayed second-order dynamical systems will satisfy stochastic delay differential equations of the form $\ddot{x}=f[x,x(t-\tau),\dot{x},\dot{x}(t-\tau)]+g(x)\Gamma(t)$, where $x(t)$ is the state variable of interest and τ corresponds to the time delay. Roughly speaking, the function f here describes the deterministic part of the dynamics, whereas the expression $g\Gamma$ describes the stochastic part and is composed of an amplitude function g and a fluctuating part $\Gamma(t)$. Our objective will be to study systems for which f is a linear function because (i) such systems are of physical relevance as argued above, (ii) systems of this kind describe linear approximations of nonlinear systems, and (iii) such systems allow us to study properties of second-order dynamical systems subjected to fluctuations in an analytical approach. As far as the stochastic part $g\Gamma$ is concerned, we are dealing with additive noise if g corresponds to a constant and with multiplicative noise if g depends explicitly on x. Additive noise can be regarded as thermal noise that arises from the contact of a system with its environment. Additive thermal noise is present in all kinds of nonisolated systems operating at finite temperatures and, in particular, in biological systems [59]. Multiplicative noise typically emerges in open systems involving fluctuating parameters and supports the functioning of a system [60]. In terms of the aforementioned examples, we see that in most studies additive noise sources have been considered. Multiplicative noise has been used to explore the origin of negative autocorrelations of time-delayed balancing movements [20] and to study delay-induced dynamical instabilities of the pupil light reflex [61]. In particular, as far as the stochastic pupil dynamics is concerned, there is nowadays both experimental and theoretical evidence that the pupil dynamics is subjected to multiplicative noise [62–64]. Moreover, there is some experimental evidence that there is a complex interaction between the synaptic noise and the firing rate of human motoneurons that is reminiscent of multiplicative noise [65]. In view of the different origins of additive and multiplicative noise, our best assumption for the time being is that complex systems are subjected to both kinds of noise sources. However, as stated earlier, most studies focus on the impact of thermal additive noise because it is reasonable to assume that this kind of noise is indeed present in most systems and because multiplicative noise systems often confront us with problems that still cannot be solved with the (analytical) techniques available so far. Therefore, in what follows, we will only consider additive noise sources.

In short, the objective of our study is to explore the stochastic behavior of linear second-order dynamical systems with time delays and additive noise that feature Hopf bifurcation points. From the theory of nondelayed dynamical systems it is clear that in systems with two degrees of freedom phenomena can be observed that are qualitatively different from those observed in systems with a single degree of freedom. Therefore, we may expect to observe phenomena in a stochastic second-order dynamical system with time delay that are not observed in a time-delayed first-order dynamical system. To anticipate, in the present study, we will show that, in the case of stochastic time-delayed second-order dynamical systems, the variance as a function of the time delay may exhibit a sequence of pronounced peaks. That is, such systems may feature delay-induced destabilization resonances.

The manuscript is organized as follows. In Sec. II, we will derive the stationary distribution of a linear second-order dynamical system involving a time delay and a fluctuating force. In Sec. III, we will discuss in detail how the variance of the stationary distribution depends on the time delay for the two cases when there are Hopf bifurcation points (Sec. III A) and when there are no Hopf bifurcation points (Sec. III B). Section IV is devoted to the phenomenon of delay-induced destabilization resonances. Implications for human motor control will be discussed in Sec. V both in terms of reinterpretations of previous experimental studies and predictions for future studies.

II. STATIONARY PROBABILITY DENSITIES

We consider the following linear stochastic delay differential equation of second order given by

$$m\ddot{x}(t) = -av(t) - bv(t-\tau) + F(x) + \sqrt{Q}\Gamma(t) \tag{1}$$

for $t>0$. For $b=0$, Eq. (1) corresponds to the Kramers equation [66]. The Kramers equation is used to describe the motion of a particle with mass m in terms of its position $x(t) \in \mathbb{R}$ and velocity $v(t)=\dot{x}(t)$ under the impact of a damping force $-av$, a conservative force $F(x)$, and a fluctuating force $\Gamma(t)$. Note that $\sqrt{Q}\Gamma(t)$ is the Langevin force with amplitude Q which satisfies $\langle\Gamma(t)\rangle=0$ and $\langle\Gamma(t)\Gamma(t')\rangle=\delta(t-t')$, where $\delta(t-t')$ is the Dirac delta function [66]. For $b>0$, Eq. (1) accounts for possible memory effects in the damping force, where τ is the time delay. For this reason, we will refer to Eq. (1) as a Kramers model with time delay. Note also that in the following, we will consider only positive damping coefficients a and b and assume that F is the conservative force of a harmonic oscillator. That is, we put $F(x)=-kx$ with $k>0$ such that Eq. (1) describes a damped harmonic oscillator with delay driven by an additive fluctuating force.

Introducing the momentum $p(t)=mv(t)$, we can rewrite the above equation as a system of first-order differential equations [78]

$$\dot{x} = \frac{p}{m}, \tag{2}$$

$$\dot{p} = -kx(t) - ap(t) - bp(t-\tau) + \sqrt{Q}\Gamma(t). \tag{3}$$

The initial condition is $x(0)=x_0$, $p(t)=\varphi(t)$ for $t\in[-\tau,0]$. In order to determine the probability density $P(x,p,t)=\langle\delta[x-x(t)]\delta[p-p(t)]\rangle$ of the random variables p and x analytically, it is helpful to note that the delay Fokker-Planck equation [43,67] that corresponds to Eqs. (2) and (3) reads

$$\frac{\partial}{\partial t}P(x,p,t) = -\frac{\partial}{\partial x}\frac{p}{m}P(x,p,t) + \frac{\partial}{\partial p}\left\{[kx+ap]P(x,p,t) + b\int_{\Omega} p_\tau P(x,p,t;p_\tau,t-\tau)dp_\tau\right\} + \frac{Q}{2}\frac{\partial^2}{\partial p^2}P(x,p,t). \tag{4}$$

Importantly, the proposed Kramers model with time delay can be solved analytically (as we will show below). Furthermore, for $k=0$, Eq. (3) corresponds to a first-order stochastic delay differential equation

$$\dot{p} = -ap(t) - bp(t-\tau) + \sqrt{Q}\Gamma(t) \tag{5}$$

that has been studied extensively in the literature (see, e.g., Refs. [14,40–46]).

A. Gaussian functions

Since Eqs. (2) and (3) are linear with respect to x and p and involve a fluctuating force Γ with Gaussian characteristic functional, we conclude that the stationary distribution $P_{st}(x,p)$ is a Gaussian function. From Eqs. (2) and (3) it is clear that the mean values of x and p vanish. Consequently, $P_{st}(x,p)$ assumes the form $P_{st}(x,p)\sim\exp[c_1x^2+c_2p^2+c_3px]$. In particular, the stationary distribution for p is the Gaussian distribution

$$P_{st}(p) = \sqrt{\frac{1}{2\pi\sigma_p^2(\tau)}}\exp\left\{-\frac{p^2}{2\sigma_p^2(\tau)}\right\}. \tag{6}$$

Note that $\sigma_p^2(\tau)$ represents the variance of p. Next, we examine the correlation between x and p. To this end, we multiply Eq. (2) with x and take the average. We then have

$$\langle x\dot{x}\rangle = \frac{\langle px\rangle}{m}. \tag{7}$$

Since in the stationary case $\langle x\dot{x}\rangle=0.5d\langle x^2\rangle/dt=0$, we get $\langle xp\rangle=0$. Consequently, x and p are uncorrelated and the stationary solution of Eq. (4) is given by

$$P_{st}(x,p) = \frac{1}{2\pi}\sqrt{\frac{1}{\sigma_p^2(\tau)\sigma_x^2(\tau)}}\exp\left\{-\left(\frac{x^2}{2\sigma_x^2}+\frac{p^2}{2\sigma_p^2}\right)\right\}. \tag{8}$$

In particular, we have $P_{st}(x,p)=P_{st}(x)P_{st}(p)$.

B. Variances

In order to obtain the explicit stationary distribution (8), analytical expressions for the variances of x and p must be derived. To this end, we use the autocorrelation technique that has been developed in previous works [40,41,48]. We introduce the stationary autocorrelation function $C(z)=\langle p(t)p(t+z)\rangle_{st}$, where $z>0$ is a parameter and $C(0)=\langle p^2(t)\rangle$ is the variance of p. We also introduce the cross-correlation function $g(z)=\langle p(t)x(t+z)\rangle_{st}$, where $g(0)=0$. Using the autocorrelation and the cross-correlation function, we can derive from the delay differential equations with noise (2) and (3) the delay differential equations without noise

$$\frac{d}{dz}g(z) = \frac{1}{m}C(z),$$

$$\frac{d}{dz}C(z) = -kg(z) - aC(z) - bC(z-\tau) \tag{9}$$

for $z>0$. Note that $\langle p(t)\Gamma(t+z)\rangle_{st}=0$ for $z>0$ because of causality [40]. Due to the symmetry property of the autocorrelation function $C(z)=C(-z)$, the system (9) can be written as

$$\frac{d}{dz}g(z) = \frac{1}{m}C(z),$$

$$\frac{d}{dz}C(z) = -kg(z) - aC(z) - bC(\tau-z). \tag{10}$$

Since $C(0)$ is the variance of p, our objective is to solve the system (10) for $C(z)$ and $g(z)$. We derive the autocorrelation function $C(z)$ and the cross-correlation function $g(z)$ by solv-

ing Eq. (10) under appropriate constraints. Obviously, the first constraint is given by

$$g(0) = 0. \tag{11}$$

Integrating the delay Fokker-Planck equation (4) in the stationary case with respect to x and exploiting $\int x P_{\mathrm{st}}(x,p)dx = \langle x \rangle_{\mathrm{st}} P_{\mathrm{st}}(p) = 0$, we obtain

$$0 = \frac{\partial}{\partial p}\left\{ apP_{\mathrm{st}}(p) + b\int_{\Omega} p_\tau P_{\mathrm{st}}(p,t;p_\tau,t-\tau)dp_\tau \right\} + \frac{Q}{2}\frac{\partial^2}{\partial p^2}P_{\mathrm{st}}(p). \tag{12}$$

Multiplying Eq. (12) with p^2 and integration with respect to p yields

$$aC(0) + bC(\tau) = \frac{Q}{2}. \tag{13}$$

Since $g(0)=0$, it follows from Eq. (9) that

$$\left.\frac{d}{dz}C(z)\right|_{z\to 0^+} = -\frac{Q}{2}. \tag{14}$$

Differentiating Eq. (10) with respect to z and taking $z \to 0^+$, we obtain

$$\left.\frac{d^2}{dz^2}C(z)\right|_{z\to 0^+} = -\frac{k}{m}C(0) - a\frac{d}{dz}C(0) + b\frac{d}{dz}C(\tau). \tag{15}$$

In order to derive the variance of x, we multiply the delay Fokker-Planck equation (4) with the product px and integrate the result with respect to x and p. Thus, we find

$$0 = \frac{1}{m}\langle p^2 \rangle_{st} - k\langle x^2 \rangle_{st} - a\langle xp \rangle_{st} - b\langle x(t)p(t-\tau) \rangle_{st}. \tag{16}$$

Since $\langle xp \rangle_{st}=0$, $\sigma_p^2 = \langle p^2 \rangle_{st}$ and $\sigma_x^2 = \langle x^2 \rangle_{st}$, from Eq. (16) we obtain

$$\sigma_x^2 = \frac{1}{k}\left[\frac{\sigma_p^2}{m} - bg(\tau) \right]. \tag{17}$$

Just as in previous works [40,41], we need to distinguish between different cases in order to solve the system (10). For $b>a$, we will use an autocorrelation function $C(z)$ in the form of sinusoidal functions. For $b<a$ and $b^2 > a^2 - (4k/m)$, we will use hyperbolic sine and cosine functions with complex-valued arguments to form $C(z)$. In contrast, for $b<a$ and $b^2 < a^2 - (4k/m)$, we will use hyperbolic sine and cosine functions with real-valued arguments. If we introduce $\gamma = \sqrt{a^2 - b^2}$ for $b<a$ as an effective damping coefficient, then we may say that the system is underdamped if $b^2 > a^2 - (4k/m) \Rightarrow \gamma^2 - (4k/m) < 0$ and overdamped if $b^2 < a^2 - (4k/m) \Rightarrow \gamma^2 - (4k/m) > 0$. In the following, we will first discuss the first case $b>a$, then the third (overdamped) case $b<a$, $a^2 - b^2 - (4k/m) < 0$, and finally the second (underdamped) case $b<a$, $a^2 - b^2 - (4k/m) > 0$.

1. Case (1): $b>a$

Suppose that

$$C(z) = A_c \cos[\omega(z - \tau/2)] + A_s \sin[\omega(z - \tau/2)], \tag{18}$$

where A_c and A_s are real constants and the parameter ω represents a frequency. To determine ω, we first calculate $g(z)$ from Eq. (10). Then, we have

$$g(z) = \frac{1}{m\omega}\{A_c \sin[\omega(z - \tau/2)] - A_s \cos[\omega(z - \tau/2)] + g_0\} \tag{19}$$

with $g_0 = A_c \sin(\omega\tau/2) + A_s \cos(\omega\tau/2)$. It follows that

$$\frac{d}{dz}C(z) = \omega\{A_s \cos[\omega(z - \tau/2)] - A_c \sin[\omega(z - \tau/2)]\}, \tag{20}$$

$$C(\tau - z) = A_c \cos[\omega(z - \tau/2)] - A_s \sin[\omega(z - \tau/2)]. \tag{21}$$

Substituting Eqs. (18)–(21) into Eq. (10) and collecting the amplitudes of the sine and cosine functions, we get

$$\omega\left(1 - \frac{k}{m\omega^2}\right)A_s = -A_c(a+b), \tag{22}$$

$$\omega\left(1 - \frac{k}{m\omega^2}\right)A_c = A_s(a-b). \tag{23}$$

Solving for ω, we obtain two frequencies

$$\omega_{1,2} = \frac{\sqrt{b^2 - a^2}}{2} \pm \sqrt{\frac{b^2 - a^2}{4} + \frac{k}{m}}. \tag{24}$$

Next, we use the superposition of the particular solutions (18) with frequencies ω_1 and ω_2 resulting in

$$C^{(1)}(z) = C_1^{(1)} \cos(\omega_1 z) + e_1^{(1)} \sin(\omega_1 z) + C_2^{(1)} \cos(\omega_2 z) + e_2^{(1)} \sin(\omega_2 z), \tag{25}$$

where $C_1^{(1)}$, $C_2^{(1)}$, $e_1^{(1)}$, and $e_2^{(1)}$ are parameters. Using the constraints (11)–(15), after some detailed calculations, we find $e_1^{(1)} = -Q\omega_1/2(\omega_1^2 - \omega_2^2)$ and $e_2^{(1)} = -e_1^{(1)}\omega_2/\omega_1$, and

$$C_1^{(1)}(\tau) = \frac{Q}{2Z^{(1)}(\tau)}\left\{ a - b\frac{\omega_1^2 \cos(\omega_1\tau) - \omega_2^2 \cos(\omega_2\tau)}{\omega_1^2 - \omega_2^2} - bB^{(1)}(\tau)\frac{b\omega_2 \sin(\omega_2\tau) - \omega_2^2 + (k/m)}{a + b\cos(\omega_2\tau)} \right\} \tag{26}$$

$$C_2^{(1)}(\tau) = \frac{bQB^{(1)}(\tau)/2 - [a + b\cos(\omega_1\tau)]C_1^{(1)}(\tau)}{a + b\cos(\omega_2\tau)}, \tag{27}$$

where

$$B^{(1)}(\tau) = \frac{1}{b} + \frac{\omega_1 \sin(\omega_1\tau) - \omega_2 \sin(\omega_2\tau)}{\omega_1^2 - \omega_2^2}, \tag{28}$$

$$Z^{(1)}(\tau) = b\omega_1 \sin(\omega_1\tau) - \omega_1^2 + (k/m) - \left\{\frac{a + b\cos(\omega_1\tau)}{a + b\cos(\omega_2\tau)}\right\} \times [b\omega_2 \sin(\omega_2\tau) - \omega_2^2 + (k/m)]. \quad (29)$$

The parameter $C_1^{(1)}(\tau)$ can equivalently be expressed as (see Appendix A)

$$C_1^{(1)}(\tau) = \frac{Q\omega_1\Omega}{2(\omega_1^2 - \omega_2^2)}\left(\frac{1 + b\Omega^{-1}\sin(\omega_1\tau)}{a + b\cos(\omega_1\tau)}\right) \quad (30)$$

with $\Omega = \sqrt{|b^2 - a^2|}$. From Eq. (25), it follows that the variance of p is

$$\sigma_p^{2(1)}(\tau) = C_1^{(1)}(\tau) + C_2^{(1)}(\tau). \quad (31)$$

The variance of x is given by Eq. (17) with $g(\tau) = g^{(1)}(\tau)$ and

$$g^{(1)}(\tau) = \frac{1}{m}\left\{\frac{C_1^{(1)}(\tau)}{\omega_1}\sin(\omega_1\tau) + \frac{C_2^{(1)}(\tau)}{\omega_2}\sin(\omega_2\tau) + \frac{Q}{2(\omega_1^2 - \omega_2^2)}[\cos(\omega_1\tau) - \cos(\omega_2\tau)]\right\}. \quad (32)$$

2. Case (3): $b < a$, $b^2 < a^2 - (4k/m)$

In this case, we have $b < a$ and $a^2 - b^2 > 4k/m$. A solution of Eq. (9) is given by

$$C(z) = A_c \cosh\left[\omega\left(z - \frac{\tau}{2}\right)\right] + A_s \sinh\left[\omega\left(z - \frac{\tau}{2}\right)\right], \quad (33)$$

which can be proven by substituting Eq. (33) into Eq. (9). In doing so, we can also determine the frequency ω and find

$$\omega_{1,2} = \frac{\sqrt{a^2 - b^2}}{2} \pm \sqrt{\frac{a^2 - b^2}{4} - \frac{k}{m}}. \quad (34)$$

Consequently, the frequencies $\omega_{1,2}$ are real-valued and the general solution of Eq. (9) can be cast into the form

$$C^{(3)}(z) = C_1^{(3)}\cosh(\omega_1 z) + e_1^{(3)}\sinh(\omega_1 z) + C_2^{(3)}\cosh(\omega_2 z) + e_2^{(3)}\sinh(\omega_2 z). \quad (35)$$

Exploring the constrains (11)–(15), we obtain $e_1^{(3)} = -Q\omega_1/2(\omega_1^2 - \omega_2^2)$ and $e_2^{(3)} = -e_1^{(3)}\omega_2/\omega_1$ and

$$C_1^{(3)}(\tau) = \frac{Q}{2Z^{(3)}(\tau)}\left\{a - b\frac{\omega_1^2\cosh(\omega_1\tau) - \omega_2^2\cosh(\omega_2\tau)}{\omega_1^2 - \omega_2^2} - bB^{(3)}(\tau)\frac{\omega_2^2 + (k/m) - b\omega_2\sinh(\omega_2\tau)}{a + b\cosh(\omega_2\tau)}\right\}, \quad (36)$$

$$C_2^{(3)}(\tau) = \frac{bQB^{(3)}(\tau)/2 - \{[a + b\cosh(\omega_1\tau)]C_1^{(2}(\tau)\}}{a + b\cosh(\omega_2\tau)} \quad (37)$$

where

$$B^{(3)}(\tau) = \frac{1}{b} + \frac{\omega_2\sinh(\omega_2\tau) - \omega_1\sinh(\omega_1\tau)}{\omega_2^2 - \omega_1^2}, \quad (38)$$

$$Z^{(3)}(\tau) = \omega_1^2 + (k/m) - b\omega_1\sinh(\omega_1\tau) - \left\{\frac{a + b\cosh(\omega_1\tau)}{a + b\cosh(\omega_2\tau)}\right\} \times [\omega_2^2 + (k/m) - b\omega_2\sinh(\omega_2\tau)]. \quad (39)$$

Note that by a detailed calculation similar to the one carried out in Appendix A, one can show that the parameter $C_1^{(3)}(\tau)$ can be transformed into

$$C_1^{(3)}(\tau) = \frac{Q\omega_1\Omega}{2(\omega_1^2 - \omega_2^2)}\left(\frac{1 + b\Omega\sinh(\omega_1\tau)}{a + b\cosh(\omega_1\tau)}\right) \quad (40)$$

with $\Omega = \sqrt{|b^2 - a^2|}$. From Eq. (35) and $\sigma_p^{2(3)} = C^{(3)}(0)$ it can be appreciated that $\sigma_p^{2(3)}$ is given by

$$\sigma_p^{2(3)}(\tau) = C_1^{(3)}(\tau) + C_2^{(3)}(\tau), \quad (41)$$

whereas $\sigma_x^{2(3)}$ is given by Eq. (17) with $g(\tau) = g^{(3)}(\tau)$ and

$$g^{(3)}(\tau) = \frac{1}{m}\left\{\frac{C_1^{(3)}(\tau)}{\omega_1}\sinh(\omega_1\tau) + \frac{C_2^{(3)}(\tau)}{\omega_2}\sinh(\omega_2\tau) + \frac{Q}{2(\omega_2^2 - \omega_1^2)}[\cosh(\omega_1\tau) - \cosh(\omega_2\tau)]\right\}. \quad (42)$$

3. Case (2): $b < a$, $b^2 > a^2 - (4k/m)$

Just as in the previous case, we have $b < a$, but now with $a^2 - b^2 < 4k/m$. Nevertheless, by substituting the autocorrelation function (33) into Eq. (9), one can show that Eq. (33) is a solution of Eq. (9). That is, we are dealing again with hyperbolic functions. However, from Eq. (34) and $a^2 - b^2 < 4k/m$, it follows that the frequencies are now complex variables. They are complex conjugates $\omega_{1,2} = u \pm vi$ with $u = \sqrt{a^2 - b^2}/2$ and $v = \sqrt{(k/m) - ([a^2 - b^2]/4)}$. A detailed analysis (see Appendix B shows that the variance of p is given by

$$\sigma_p^{2(2)}(\tau) = -\frac{Q}{4uvA_1}\{A_2A_3 + b\sinh(u\tau)\sin(v\tau)A_4\}, \quad (43)$$

where $A_1, \ldots, A_4$ are functions that depend on τ like

$$A_i = A_i[\cos(v\tau), \sin(v\tau), \cosh(v\tau), \sinh(v\tau)]. \quad (44)$$

The variance of x is given by Eq. (17) with $g(\tau) = g^{(2)}(\tau)$ and

$$g^{(2)}(\tau) = \frac{1}{m}\left(2\,\mathrm{Re}\left\{\frac{C_1^{(2)}\sinh(\omega_1\tau)}{\omega_1}\right\} - \frac{Q}{4uv}\sinh(u\tau)\sin(v\tau)\right). \quad (45)$$

Note that $\mathrm{Re}\{\cdots\}$ is the real part of $\{\cdots\}$.

4. Special cases

Finally, we can derive the variances σ_p^2 and σ_x^2 for the special cases $a = b$ and $k = 0$, see Appendix C. In particular, for $k = 0$, we reobtain the results that were previously derived for the first-order delay differential equation (5).

5. Examples

At this juncture it is useful to illustrate the stationary probability densities $P_{st}(p)$ and $P_{st}(x)$ for fixed parameters m,

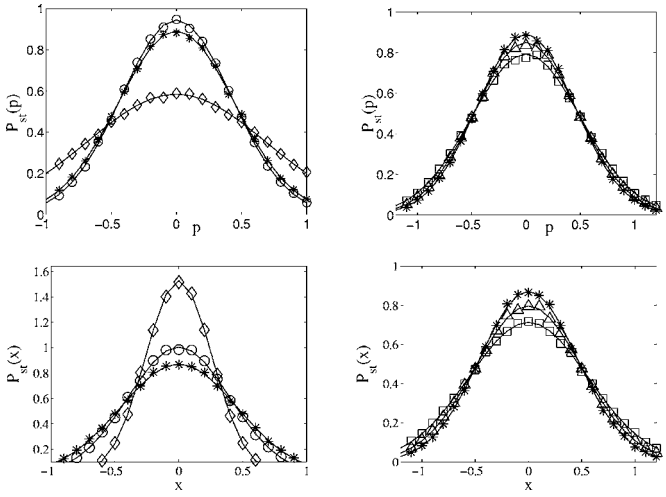

FIG. 2. Stationary probability densities of the system (2) and (3) represented by various values of parameter b while the other parameters are fixed. Symbols represent the numerical simulation and the solid lines represent the analytical results given by Eq. (8). The parameters are fixed by $a=2$, $k=0.8$, $\tau=0.2$, $Q=1$, and $m=1$. Using $b=8,2,1$, the left panels show the stationary probability densities which, for the b values used, correspond to $b>a$ (diamonds), $b=a$ (circles), and $a^2>b^2>a^2-(4/km)$ (stars), respectively. Using $b=1,0.5,0$, the right panels show the stationary probability densities which, for the b values used, correspond to $a^2>b^2>a^2-(4k/m)$ (stars), $b^2<a^2-(4k/m)$ (triangles), and $b=0$ (squares), respectively.

k, a, and τ and for several values of b. To this end, we use the analytical expressions derived in the preceding and results obtained from numerical simulations. As far as the numerics is concerned, we solved the Kramers equations (2) and (3) by an Euler forward method [66]. In the simulation, the random variables x and p were generated using a fixed time step of 10^{-2}. The fluctuating force Γ was calculated based on a Gaussian random generator (Box-Muller algorithms). The simulations were carried out for 10^5 realizations and 10^4 integration steps for each realization. The results shown in Fig. 2 represent the cases $b>a$, $b=a$, $a^2>b^2>a^2-(4k/m)$, and $b^2<a^2-(4k/m)$, respectively.

III. CRITICAL DELAYS AND LONG TIME DELAYS

We consider the delay as the control parameter of the system (2) and (3). The objective is to study the impact of this control parameter on the dynamical behavior of the system (2) and (3). For $b>a$, the stability is determined by critical delays at which Hopf bifurcations occur. In contrast, for $b<a$ there are no Hopf bifurcations.

A. Critical delays, Hopf bifurcations, and double Hopf bifurcations

1. Deterministic system

The deterministic equations that correspond to the Kramers equations (2) and (3) for $Q=0$ are given by

$$\dot{x} = \frac{p}{m}, \tag{46}$$

$$\dot{p} = -kx(t) - ap(t) - bp(t-\tau). \tag{47}$$

Such second-order dynamical systems with time delays have been studied in detail, for example, in Refs. [52,53]. The specific second-order dynamical model given by Eqs. (46) and (47) has been analyzed in Refs. [68–70]. Let λ be an eigenvalue of the system. The characteristic equation [19] is then defined by

$$\lambda^2 + a\lambda + \frac{k}{m} + b\lambda \exp(-\lambda\tau) = 0. \tag{48}$$

The stability is changed due to a Hopf bifurcation if there is a critical delay τ_c such that $\lambda=\omega i$ is a purely imaginary root of Eq. (48), where ω is a positive real value. Substituting $\lambda=\omega i$ into Eq. (48), we find

$$\cos(\omega\tau) = -\frac{a}{b}, \quad \omega b \sin(\omega\tau) = \omega^2 - \frac{k}{m}. \tag{49}$$

For $a>b\geqslant 0$, it has been shown that all roots λ of Eq. (48) have negative real parts for all τ [68–70]. That is, critical delays do not exist.

Next, let us consider the case $b\geqslant a$. In this case, the critical delays at which purely imaginary roots of Eq. (48) exist are given by [68–70]

$$\tau_c = \begin{cases} \tau_{u,j} = \dfrac{1}{\omega_1}\left[2j\pi + \arccos\left(-\dfrac{a}{b}\right)\right], & \omega_1^2 - (k/m) > 0 \\ \tau_{s,j} = \dfrac{1}{|\omega_2|}\left[(2j+2)\pi - \arccos\left(-\dfrac{a}{b}\right)\right], & \omega_2^2 - (k/m) < 0 \end{cases} \tag{50}$$

with $j=0,1,2,3,\ldots$ and $\lambda_{1,2}=i\omega_{1,2}$, where the Hopf frequencies $\omega_{1,2}$ are defined by Eq. (24). Furthermore, it has been shown that the delays $\tau_{u,i}$ and $\tau_{s,i}$ constitute a monotonically increasing sequence of real numbers

$$\tau_{u,0} < \tau_{s,0} < \tau_{u,1} < \tau_{s,1} < \cdots < \tau_{u,n-1} < \tau_{s,n-1} < \tau_{u,n} \tag{51}$$

up to a particular integer n. For instance, in Fig. 3, we plot $\tau_{u,i}$ and $\tau_{s,i}$ for fixed parameters b, k, and m as a function of the parameter a. The structure of the resulting diagram has been referred to as a "Christmas tree" [53,71]. In Fig. 3 (left panel) for relatively small parameters a with $a<a_1^*\approx 1.46$, we have $n=0$ [i.e., the inequality (51) consists only of $\tau_{u,0}$]. For intermediate parameters a with $a_1^*<a<a_2^*\approx 1.57$, we have $n=1$ [i.e., the inequality (51) consists of $\tau_{u,0},\tau_{s,1},\tau_{u,1}$], see also panel (b) of Fig. 3. For relatively large parameters a with $a_2^*<a<b$, we have $n=2$, see Fig. 3(b). In the limit $a\rightarrow b-0$, the upper and lower branches of τ_c given by $\tau_{u,j}$ and $\tau_{s,j}$ converge to

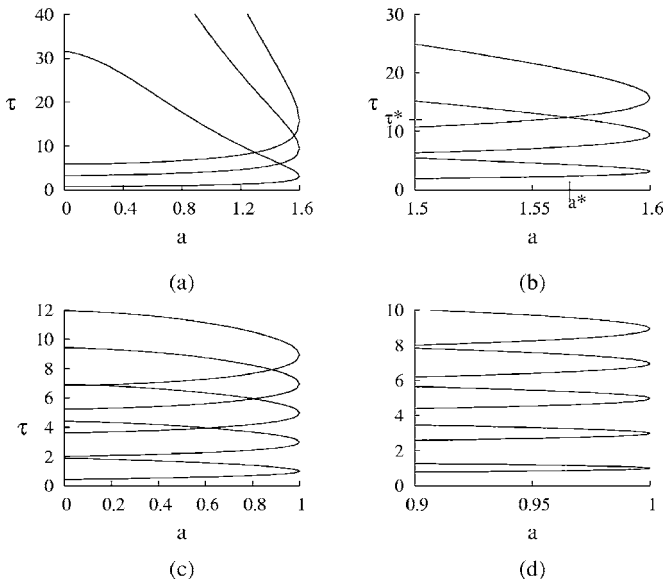

FIG. 3. Stability diagram in the a-τ plane for the case $b>a$. Panel (a): the parameters $Q=m=k=1$ and $b=1.6$ are fixed, whereas the parameter a is varied from 0 to b. Three double Hopf bifurcation points can be found at approximately (1.30, 8.53), (1.46, 5.98), and (1.57, 12.39). Panel (b): a detail of panel (a) for $a\in[1.5,1.6]$. Panel (c): stability diagram revealing (right hand side) boundary points given by $a\to b-0$ and $\tau_c=\pi(1+2j)/\omega_0$. Parameters: $Q=m=b=1$ and $k=10$. Panel (d): a detail of panel (c).

$$\tau_c(a=b)=\tau_{u,j}=\tau_{s,j}=\frac{\pi(1+2j)}{\omega_0} \tag{52}$$

with $j=0,1,2,3,\ldots$ and $\omega_0=\sqrt{k/m}$. That is, the right hand side boundary of a stability diagram in the a-τ plane consists of a set of vertically arranged and equally spaced points $(b,T_0/2)$, $(b,3T_0/2)$, $(b,5T_0/2)$, … with $T_0=(2\pi)/\omega_0$, see panels (c) and (d) in Fig. 3. These "ladder points" are closely related to the destabilization resonances that will be discussed below.

For $\tau\in\{\tau_{u,j}\}$ and $\omega=\omega_1$, it has been shown that $d\,\mathrm{Re}(\lambda)/d\tau>0$ [69]. That is, all roots of Eq. (48) cross the imaginary axis from left to right. Conversely, for $\tau\in\{\tau_{s,j}\}$ and $\omega=|\omega_2|$, the relation $d\,\mathrm{Re}(\lambda)/d\tau<0$ holds. That is, all roots of Eq. (48) cross the imaginary axis from right to left. With these results in hand, one can determine the stable regions of the fixed point $(x,p)=(0,0)$. The fixed point is stable for delays τ with $0<\tau<\tau_{u,0}$ and $\tau_{s,j}<\tau<\tau_{u,j+1}$ for $j<n$, and unstable for delays τ with $\tau_{u,j}<\tau<\tau_{s,j}$ for $j<n$ [68–70]. For $\tau>\tau_{u,n}$, the fixed point is unstable and does not become stable again. Roughly speaking, the fixed point becomes unstable at critical delays $\tau_{u,j}$ and stable again at critical delays $\tau_{s,j}$.

From inequality (51), it follows that the stability of the fixed point switches $2n+1$ times as τ is increased. In other words, as the time delay is increased, we observe a destabilization, then a restabilization, then a destabilization, and so on. As illustrated in Refs. [52,53], the sequence of stability switches breaks off due to double Hopf bifurcation points. From Eq. (50), it follows that the Hopf frequencies ω_1 and $|\omega_2|$ become equivalent if the two branches of the Hopf bifurcation points shown in Fig. 3 intersect. That is, if we have $\tau_{u,j+1}=\tau_{s,j}$ for a particular parameter a. In Fig. 3(a), such double Hopf bifurcation points are shown. Two of them can be used to distinguish between parameter domains for which one, three, or five switches in stability occur.

2. Stochastic system

It is known that stationary distributions of linear stochastic delay differential equations, such as the Kramers equations (2) and (3), exist if and only if all roots of the characteristic equation (48) have negative real parts [41,44,47]. Consequently, for $a>b$ stationary distributions of the system (2) and (3) exist for all $\tau\geqslant 0$. For $b>a$, stationary distributions exist for delays τ for which $0\leqslant\tau<\tau_{u,0}$ or $\tau_{s,j}<\tau<\tau_{u,j+1}$ hold, with $j<n$. Otherwise, they do not exist. In particular, the moments $\langle x\rangle$ and $\langle p\rangle$ of Eqs. (2) and (3) satisfy the evolution equations (46) and (47). Consequently, the stable stationary points $\langle x\rangle_{\mathrm{st}}=\langle p\rangle_{\mathrm{st}}=0$ of these evolution equations become unstable at the critical delays $\tau_{u,j}$ and stable again at critical delays $\tau_{s,j}$ for $j=0,1,\ldots,n$.

3. Variances

Here we restrict ourselves to the case $b>a$. We will show that the variances σ_p^2 and σ_x^2 become infinite at the critical delays $\tau_{u,j}$ for $j\leqslant n$ and become finite at critical delays $\tau_{s,j}$ for $j<n$. In this case, we are dealing with the variances given by Eqs. (17) and (31). First, we note that from Eq. (30) it can be appreciated that $C_1^{(1)}(\tau)$ becomes infinite for

$$\tau^*=\frac{1}{\omega_1}\arccos\left(-\frac{a}{b}\right). \tag{53}$$

Since $|\omega_2|<\omega_1$, it follows that the denominator $a+b\cos(\omega_2\tau)$ of Eq. (27) is different from zero for $[0,\tau^*]$. Therefore, $C_2^{(1)}(\tau)$ is finite for $[0,\tau^*)$. For $\tau\to\tau^*$, the parameter $C_2^{(1)}(\tau)$ is still finite. The reason for this is that $C_1^{(1)}(\tau)$ tends to infinity for $\tau\to\tau^*$ like $1/[a+b\cos(\omega_1\tau)]$, which implies that the product $[a+b\cos(\omega_1\tau)]C_1^{(1)}(\tau)$ is finite for $\tau\to\tau^*$. In sum, in the limit $\tau\to\tau^*$ the variance $\sigma_2^{2(1)}(\tau)=C_1^{(1)}\times(\tau)+C_2^{(1)}(\tau)$ tends to infinity because $C_1^{(1)}(\tau)$ tends to infinity and $C_2^{(1)}(\tau)$ is finite. Comparing Eqs. (50) and (53), we see that $\tau^*=\tau_{u,0}$. The same argument holds for critical delays $\tau_{u,j}$ for $0<j\leqslant n$. In the limit $\tau\to\tau_{u,j}-0$, the parameter $C_2^{(1)}\times(\tau)$ is finite but the parameter $C_1^{(1)}(\tau)$ becomes infinite, which implies that $\sigma_2^{2(1)}(\tau)$ tends to infinity. We now turn to the critical delays $\tau_{s,j}$. Using Eq. (27), we see that the parameter $C_2^{(1)}(\tau)$ is proportional to $1/[a+b\cos(\omega_2\tau)]$. By a similar reasoning, we conclude that in the limit $\tau\to\tau_{s,j}+0$ the parameter $C_1^{(1)}(\tau)$ is finite but the parameter $C_2^{(1)}(\tau)$ becomes infinite. Consequently, if the system is in a parameter domain with a finite variance and we decrease the delay toward a critical delay $\tau_{s,j}$, then the variance $\sigma_p^{2(1)}(\tau)$ tends to infinity. It is useful to elucidate the divergence of the variances σ_p^2 and σ_x^2 at the critical delay $\tau_c=\tau_{u,0}$ with an example (illustrations of the behavior for $\tau>\tau_{u,0}$ will be presented in Sec. IV). In Fig. 4, the variances σ_p^2 and σ_x^2 have been plotted as

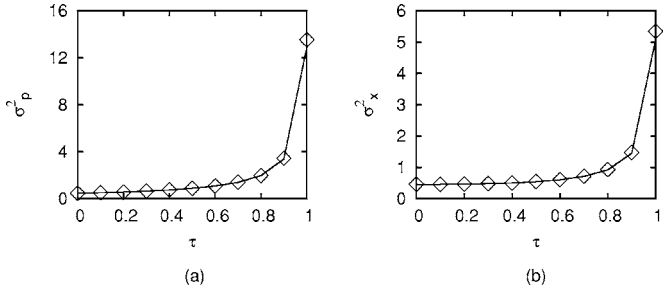

FIG. 4. Variances for the case $b>a$ versus delay. The diamonds show simulation results and the lines show analytical results given by Eqs. (17) and (31). The parameters are $a=0.1$ and $b=k=m=Q=1$, which implies that the critical delay is about 1.04.

functions of the delay τ for a system with $b>a$. Both analytical and numerical results are shown. In Fig. 4, the divergence of the variances in the limit $\tau\to\tau_{u,0}$ is clearly visible [79].

Finally, we consider the special case $b=a$. For $b=a$, we see from Eq. (C8) that at

$$\tau^* = \frac{\pi}{\omega_0}(1+2j) \tag{54}$$

with $j=0,1,2,3,\ldots$ the variance σ_p^2 becomes infinite. Furthermore, from Eq. (C9) it then follows that σ_x^2 becomes infinite for $\tau=\tau^*$. Comparing Eqs. (52) and (54), we see that the equivalence $\tau^*=\tau_c$ holds, which means that the variances become infinite at the critical delays of the deterministic system. In Fig. 5, we give an example of the behavior of a system with $b=a$ at the first critical delay $\tau_c=\pi/\omega_0$. We see that the variances σ_p^2 and σ_x^2 are monotonically increasing functions of the delay τ and tend to infinity for $\tau\to\tau_c$.

B. Long time delays

As argued in Sec. III A, there is no critical delay if $a>b$, which implies that stationary distributions of the Kramers equations (2) and (3) exist for arbitrary delays and the variances σ_p^2 and σ_x^2 are finite. In fact, for $b^2<a^2-(4k/m)$, the limit of the variances for $\tau\to\infty$ can be calculated analytically. To this end, we replace $\sinh(\omega_i\tau)$ and $\cosh(\omega_i\tau)$ by $\exp(\omega_i\tau)/2$ for $i=1,2$ in Eqs. (36), (37), and (43). Thus, we obtain

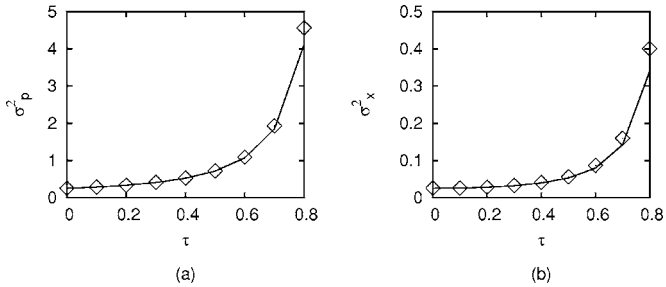

FIG. 5. Variances for the case $b=a$ versus delay. The diamonds show simulation results and the lines show analytical results given by Eqs. (C8) and (C9). The parameters are $a=b=Q=m=1$ and $k=10$, which yields a critical delay of about 0.99.

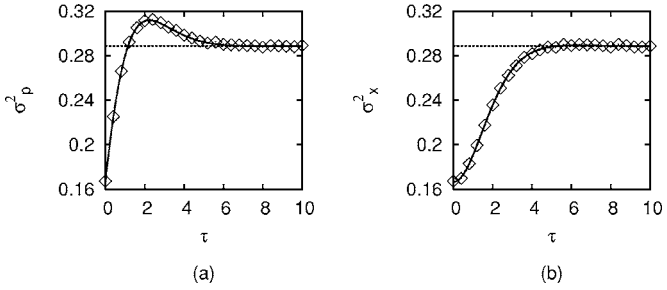

FIG. 6. Variances at large delays for the underdamped case with $b<a$ and $b^2>a^2-(4k/m)$. The diamonds show the simulation results and the lines show the analytical results given by Eqs. (17), (43), and (45). Parameters: $a=2$ and $b=k=m=Q=1$.

$$\lim_{\tau\to\infty}\sigma_p^{2(3)}(\tau) = \frac{Q}{2(\omega_1+\omega_2)}. \tag{55}$$

Using this result, from Eqs. (17), (42), and (45) the limit $\sigma_x^{2(3)}$ for $\tau\to\infty$ reads

$$\lim_{\tau\to\infty}\sigma_x^{2(3)}(\tau) = \frac{Q}{2km(\omega_1+\omega_2)}. \tag{56}$$

Substituting in Eqs. (55) and (56) the complex frequencies $\omega_{1,2}=u\pm iv$ introduced in Sec. II B, we obtain for the case $a^2>b^2>a^2-(4k/m)$, the asymptotic values

$$\lim_{\tau\to\infty}\sigma_p^{2(2)}(\tau) = \frac{Q}{2\Omega} \tag{57}$$

and

$$\lim_{\tau\to\infty}\sigma_x^{2(2)}(\tau) = \frac{Q}{2km\Omega} \tag{58}$$

with $\Omega=\sqrt{|b^2-a^2|}$. In Figs. 6 and 7, both analytical and numerical results for the variances σ_p^2 and σ_x^2 and the asymptotic values computed from Eqs. (55)–(58) are plotted for $a^2>b^2>a^2-(4k/m)$ and $b^2<a^2-(4k/m)$, respectively. From these figures, it is evident that for $\tau\to\infty$ the variances of x and p approach finite asymptotic values that are given by Eqs. (55)–(58).

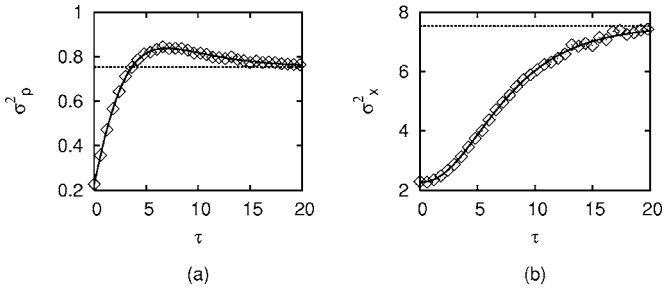

FIG. 7. Asymptotic behavior of the variances for the overdamped case with $b<a$ and $b^2<a^2+(4k/m)$. The diamonds show the simulation results and the lines show the analytical results given by Eqs. (17), (41), and (42). Parameters: $a=1.2$, $b=m=Q=1$, and $k=0.1$.

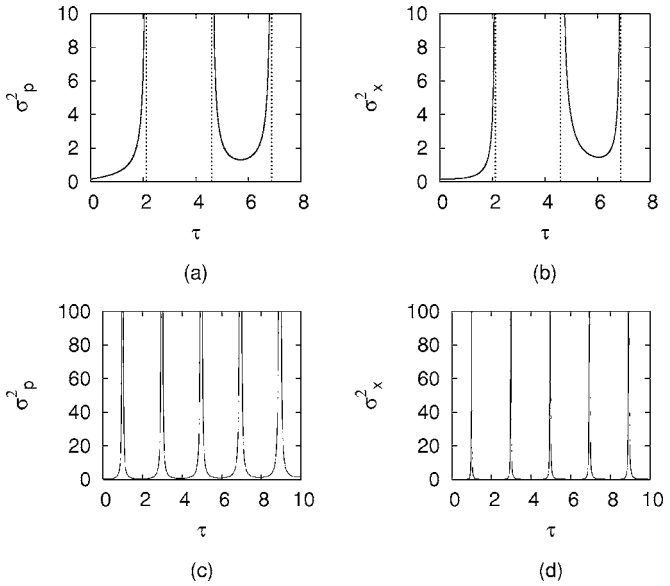

FIG. 8. (a) Variance of p and (b) variance of x for $b>a$ in the case of a re-entrant bifurcation. There are two stable domains in which the variance is finite: $[0,\tau_{u,0})$ and $(\tau_{s,0},\tau_{u,1})$. For $\tau \geqslant \tau_{u,1}$ stationary distributions do not exist. Vertical bars correspond to $\tau_{u,0}$, $\tau_{s,0}$, and $\tau_{u,1}$. The parameters: $a=1.5$, $b=1.6$, and $Q=m=k=1$. (c) Variance of p and (d) variance of x for $b=a$. Singularities occur at regular intervals. Parameters: $a=b=Q=m=1$ and $k=10$.

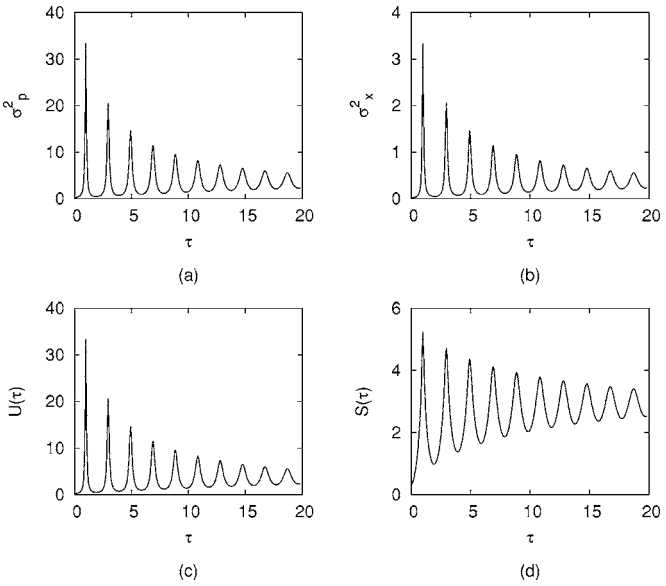

FIG. 9. (a) Variance of p, (b) variance of x, (c) energy $U(\tau)$, and (d) entropy $S(\tau)$ with respect to time delay for the underdamped case with $b<a$ and $b^2>a^2-(4k/m)$. Parameters: $a=1.01$, $b=Q=m=1$, and $k=10$.

IV. DELAY-INDUCED DESTABILIZATION RESONANCES

A. Destabilization resonances due to oscillatory ghost instabilities: connections with "Christmas tree" stability diagrams

As stated earlier, from Eqs. (26) and (27) [as well as from Eqs. (C8) and (C9)], we see that for $b \geqslant a$ the variances σ_p^2 and σ_x^2 are composed of trigonometric functions given by $\cos(\omega_i \tau)$ and $\sin(\omega_i \tau)$ with $i=1,2$. This implies that for $b \geqslant a$, the variances σ_p^2 and σ_x^2 exhibit some kind of oscillatory behavior. This oscillatory behavior, however, is only relevant in the stability domains $0<\tau<\tau_{u,0}$ and $\tau_{s,j}<\tau<\tau_{u,j+1}$ for $j<n$. In order to reveal the oscillatory properties of the variances $\sigma_p^2(\tau)$ and $\sigma_x^2(\tau)$, we may plot them for delays larger than $\tau_{u,0}$. Figure 8 illustrates a system for $b>a$ involving two stability domains. The rising edge in the second stability domain can be regarded as some kind of periodic repetition of the rising edge of the first stability domain. The two stability domains correspond to the stability domains revealed by the Christmas tree stability diagram shown in panel (b) of Fig. 3 . That is, if we increase the time delay along the y axis of the diagram in panel (b) of Fig. 3, we drive the deterministic system through a sequence of destabilization and restabilization points. Simultaneously, as shown in panels (a) and (b) of Fig. 8 , we drive the variances σ_x^2 and σ_p^2 of the corresponding stochastic system through a sequence of singularities that mark off the parameter domains in which stationary distributions exist.

Figure 8 also illustrates a time-delayed system for $b=a$. As shown in panels (c) and (d) [and as we anticipate from Eqs. (C8) and (C9)] the variances σ_p^2 and σ_x^2 are periodic functions with a period $T_0=2\pi/\omega_0$. Singularities correspond to the critical delays $\tau_c=(1+2j)T_0/2$ defined by Eq. (52). These singularities correspond to the ladder points that constitute the right hand boundary of the Christmas tree stability diagram shown in Fig. 3(d).

Next we consider the underdamped case. For parameters a and b that satisfy $b<a$ but are still located close to the bifurcation line $b=a$ in the parameter space (a,b), we obtain variances with very pronounced oscillations, see Fig. 9 . Comparing Figs. 8 and 9, we see that the peaks shown in Fig. 9 are remnants or ghosts of the singularities shown in Fig. 8(b) and identify points in the parameter space (a,b,τ,k,m) where certain matching conditions are satisfied. Consequently, we may refer to them as resonances. Since they represent maxima of the variances σ_p^2 and σ_x^2, they describe conditions of maximal destabilization and may be referred to as destabilization resonances. The destabilization resonances are related to the oscillatory instability points (Hopf bifurcation points) that exist in the parameter domain $b \geqslant a$. For this reason, we may say that the destabilization resonances are due to oscillatory ghost instabilities [80]. Alternatively, a simple interpretation of the resonance peaks can be given in terms of the Christmas tree diagrams of the corresponding deterministic systems. Accordingly, the peaks are the remnants of the ladder points $[b,(1+2j)T_0/2]$ with $j=0,1,2,3,\ldots$.

It should be mentioned that for $k=0$, destabilization resonances cannot be observed (see also Fig. 1). Therefore, we may say that they are caused by the influence of the restoring force $-kx$. This becomes also clear from Eq. (34) because for $b \approx a$ the frequencies $\omega_{1,2}$ can be expressed in terms of $\omega_0=\sqrt{k/m}$. That is, the frequencies are dominated by the parameter k and the restoring force $-kx$.

The envelope of the oscillatory behavior of the functions σ_p^2 and σ_x^2 for $a^2>b^2>a^2-(4k/m)$ is determined by the

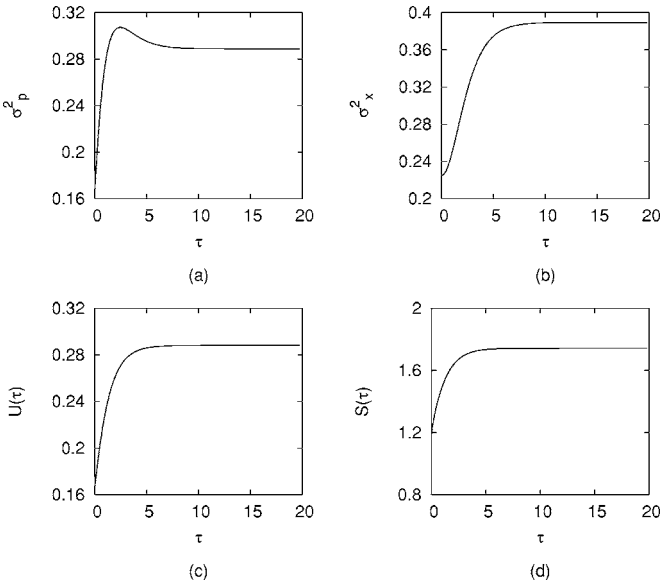

FIG. 10. (a) Variance of p, (b) variance of x, (c) energy $U(\tau)$, and (d) entropy $S(\tau)$ with respect to time delay for the overdamped case with $b<a$ and $b^2<a^2-(4k/m)$. Parameters: $a=2$, $b=Q=m=1$, and $k=0.74$.

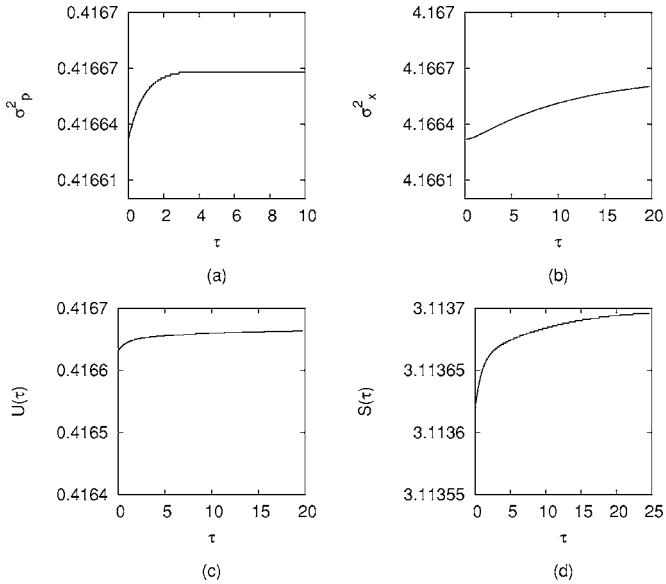

FIG. 11. (a) Variance of p, (b) variance of x, (c) energy $U(\tau)$, and (d) entropy $S(\tau)$ with respect to time delay for the overdamped case $b<a$, $b^2<a^2-(4k/m)$. The parameters: $Q=1$, $m=1$, $k=0.1$, $a=1.2$, and $b=0.0001$.

$\sinh(u\tau)$ and $\cosh(u\tau)$ terms occurring in Eqs. (43) and (44). If the parameters b and a deviate further from the critical line $b=a$, that is, if we continue to decrease b to a fixed value of a, then the hyperbolic functions become more dominant such that the oscillatory behavior vanishes and we are left with variances σ_p^2 and σ_x^2 that look qualitatively as shown in Fig. 10: the variance σ_p^2 still exhibits a maximum but there are no further peaks as shown in panel (a) of Fig. 9. In view of the presence of a maximum, we may say that the variance is characterized by an overshoot. Such an overshoot does not require that the expression for σ_p^2 involves trigonometric functions. As shown in Fig. 10, in the overdamped case, that is, for $b^2<a^2-(4k/m)$, we also observe an overshoot in the graph of the variance σ_p^2, although the function $\sigma_p^2(\tau)$ does not involve trigonometric functions, see Eqs. (36)–(39). Finally, when the impact of the time-delayed feedback loop becomes small, then it seems that the overshoot behavior vanishes and the variances σ_p^2 and σ_x^2 increase monotonically with the time delay, see Fig. 11.

B. Energy and entropy

The characteristic features of the variances σ_p^2 and σ_x^2 carry over to the mean energy $U=\langle p^2/(2m)+kx^2/2\rangle$ and to the entropy $S=-\int P \ln P dxdp$ of the time-delayed systems given by Eqs. (2) and (3) (note that we put the Boltzmann constant equal to unity). Using the Gaussian distribution (8), we get

$$U(\tau)=\left\langle \frac{kx^2}{2}\right\rangle+\left\langle \frac{p^2}{2m}\right\rangle=\frac{k\sigma_x^2}{2}+\frac{\sigma_p^2}{2m} \tag{59}$$

and

$$S(\tau)=-\int P_{\mathrm{st}}(x,p)\ln P_{\mathrm{st}}(x,p)dpdx=1+\ln 2\pi+\ln\sqrt{\sigma_x^2\sigma_p^2}. \tag{60}$$

Accordingly, the resonance peaks of σ_p^2 and σ_x^2 correspond to peaks in the functions U and S, see Fig. 9. Likewise, overshoots can also be found in the functions U and S, see, for example, Fig. 10. Finally, when the impact of the delay term becomes small, it seems that mean energy and entropy increase monotonically with the time delay, see Fig. 11.

V. IMPLICATIONS FOR HUMAN MOTOR CONTROL

As stated in the introduction, there are various human motor control systems that can be regarded as time-delayed second-order dynamical systems. In view of the theoretical results discussed in the previous sections, we will re-evaluate some experimental results that have been obtained in previous studies on human motor control and derive predictions for future studies. Inevitably, this section has a speculative character because previous experiments were not conducted to test hypotheses derived from the Kramers model (2) and (3), while hypotheses for possible future studies are speculative by definition.

A. Reinterpretations of previous human motor control studies

In what follows, we will re-evaluate experimental data of two experiments on human tracking with time-delayed visual input carried out by Tass *et al.* [15] and Langenberg *et al.* [16], respectively. The experimental setup is essentially as follows. A subject sits in front of a screen on which a moving target is displayed that oscillates with a frequency f. The subject's task is to track the target with the arm by perform-

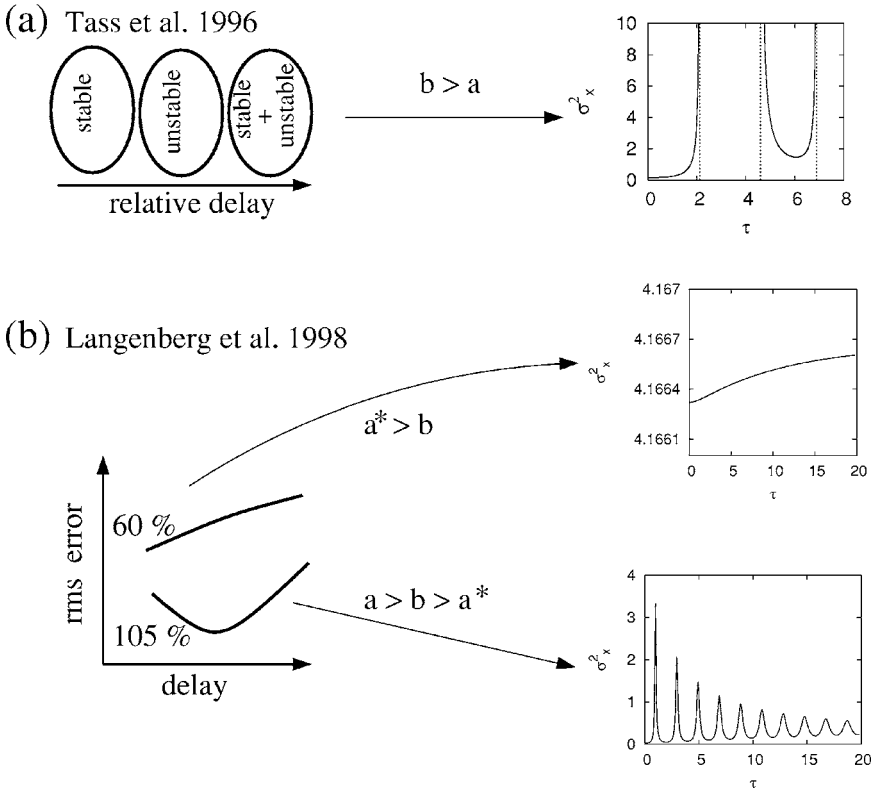

FIG. 12. Reinterpretation of experimental results found in two previous studies on tracking movements under time-delayed visual feedback: a study by Tass *et al.* [15] (a) and a study by Langenberg *et al.* [16] (b). Here, $a^* = \sqrt{a^2 - 4k/m}$. See text for details.

ing oscillatory arm movements. Vision of hand and arm is excluded. However, the arm position is displayed on the screen and the subject needs to match the feedback signal with the target signal. In order to manipulate the time delay involved in the visual feedback, the display of the arm position is retarded by a delay τ. That is, the feedback signal displayed at time t corresponds to the arm position at time $t-\tau$. The tracking movements are described in terms of the phase difference given by the difference of the phase of the feedback signal and the phase of the target signal.

Tass *et al.* found qualitatively different dynamical behaviors of tracking movements for different delays. For small time delays, tracking movements could be explained by means of a dynamical system with a stable fixed point (regime labeled (i) in Ref. [15]). For time delays larger than particular critical delays tracking movements could be regarded as the outcomes of a dynamical system exhibiting an unstable fixed point and various attractors such as limit cycles, chaotic attractors, and running solutions (regimes labeled (ii) and (iii) in Ref. [15]). For even larger time delays, Tass *et al.* found that tracking movements were related to a dynamical system that exhibits stable fixed points in some trials and unstable fixed points in others (regime labeled (iv) in Ref. [15]). These results are summarized in Fig. 12(a) . While Tass *et al.* explained these findings in terms of a nonlinear delay differential equation that is of first order in time, one may alternatively interpret the results in terms of the Kramers model (2) and (3). Accordingly, the transitions between stable and unstable fixed points found in some trials may result from an error dynamics that satisfies Eqs. (2) and (3) and operates in the parameter domain $b > a$. As illustrated in Fig. 12(a), a delay-induced sequence of destabilization and restabilization of a motor control system is at the heart of the second-order dynamical time-delayed model (2) and (3). The fact that only in some trails a restabilization was observed in the experiment by Tass *et al.* have been caused by nonlinearities that are not accounted for by the model (2) and (3). Alternatively, one may assume that the parameters of the model (2) and (3) and, in particular, the parameters a and b, vary on a slow time scale. That is, they may vary from trial to trial, such that in some trials delay-induced re-entrant transitions to stable fixed points could be observed but not in others.

Langenberg *et al.* studied how the variability of tracking movements depends on the time delay of the visual feedback. The variability was measured in terms of the root mean square (RMS) error. For small movement angles, we can assume that the RMS is proportional to the variance of the position x of the model (2) and (3) provided that Eqs. (2) and (3) describe the error dynamics of the tracking movements. Langenberg *et al.* primarily focused on the relationship between variability and the relative delay defined by the delay divided by the period of the target oscillation. It is clear from the experimental setup that the variability must become minimal if the delay is an integer multiple of the period, that is, if the relative delay is 100 percent of the period of the target oscillation, 200 percent, and so on. These kinds of variability minima are induced by the relative delay and are peculiarities of oscillatory tracking dynamics. Given our interpretation of Eqs. (2) and (3) as a model for error dynamics, we are primarily interested in an effect of the absolute time delay on performance variability. Since Langenberg *et al.* also varied the tracking frequency, they reported, as a by-product of their study, the effect of the absolute time delay on the variability. For a fixed relative delay, they evaluated the tracking movements for different target frequencies,

that is, for different absolute time delays. Fig. 12 (b) summarizes the experimental findings for this case. For a fixed relative delay of 60 percent, they found that the variability increased as a function of the absolute time delay. For a fixed relative delay of 105 percent, they found that the variability exhibits a minimum at a particular absolute time delay. Both findings can easily be explained in terms of the time-delayed Kramers model (2) and (3). Accordingly, in the case of the 60 percent condition, Langenberg *et al.* observed the error dynamics (2) and (3) for parameters a and b with $b<a^*$ and $a^*=\sqrt{a^2-(4k/m)}$. In contrast, in the case of the 105 percent condition, the error dynamics (2) and (3) for $a>b>a^*$ was observed.

In sum, our re-evaluation demonstrates that some basic experimental observations reported in the literature on time-delayed tracking movements can be related to the three qualitatively different parameter regimes of the Kramers model (2) and (3). We would like to reiterate, however, that this re-evaluation needs to be confirmed by future studies that are tailored to test the specific hypothesis made by the time-delayed Kramers model (2) and (3) when interpreted as a model for the error dynamics of tracking movements. Therefore, we will discuss next some predictions for further studies on human motor control that can be derived from the Kramers model (2) and (3).

B. Predictions for future human motor control studies

1. Time-delayed systems with $b \geqslant a$: re-entrant bifurcations and divergences

When the time delay τ is gradually increased, the deterministic second-order dynamical system given by Eqs. (46) and (47) can undergo a sequence of bifurcations. It can become unstable at critical delays $\tau_{u,j}$ and stable again at delays $\tau_{s,j}$. In such a case, we are dealing with re-entrant bifurcations. Our previous analysis has shown that at the boundaries of the stability domains, the variability of the corresponding stochastic system defined by our Kramers model (2) and (3) diverges. The implications of this observation are at least twofold.

First, the stability of human motor control systems is often determined by studying simultaneously the variability of the systems in the unperturbed stationary case and the response of the systems to perturbations [72–75]. Our analysis links these two properties, at least qualitatively. While the relaxation dynamics is related by the real parts of the eigenvalues that can be computed from the characteristic equation (48), the variability can be expressed in terms of the variances σ_p^2 and σ_x^2. Since the variances diverge when there is an eigenvalue with vanishing real part, we conclude that close to Hopf bifurcation points changes in the control parameter τ imply that either the relaxation dynamics slows down and the variability increases or the relaxation dynamics becomes faster and the variability decreases. That is, there is a strong negative correlation between the decay rate of perturbations and the variability. In fact, such a negative correlation is well known for nondelayed systems. Here, critical slowing down and critical fluctuations, two generic aspects of equilibrium and nonequilibrium phase transitions [59], usually occur simultaneously.

The second important issue concerns the phenomenon of critical fluctuations in the context of nonlinear time-delayed motor control systems. Close to stable fixed points, nonlinear systems may be studied in terms of their linearized counterparts. The evolution equations of such linearized time-delayed motor control systems may correspond to Eqs. (2) and (3). Our analysis then predicts that at the Hopf instability points, the variances of the linearized systems tend to infinity. This result will carry over to the original nonlinear systems. However, just as in the case of dynamical systems without delays [59], if nonlinearities come into play, the variances may not diverge. In sum, in the case of nonlinear time-delayed motor control systems, the variances σ_p^2 and σ_x^2 are likely to increase dramatically at Hopf bifurcation points although they are unlikely to become infinite.

2. Time-delayed systems with $b<a$: resonances and overshoots

Our results also have several important implications for time-delayed human motor control systems that are stable for all time delays $\tau \geqslant 0$. First, the "rule of thumb" which states that increasing the time delay of a system makes the system more unstable and increases the variability has been falsified. Increasing a time delay may result in an increase or a decrease of the performance variability when measured in terms of the variances σ_p^2 and σ_x^2.

Second, for systems that exhibit destabilization resonances, we conclude that the performance accuracy becomes sensitive to the time delays involved. That is, small changes in the magnitudes of the time delays can lead to large changes in performance accuracy and variability. Consequently, performance can become highly sensitive to all factors that determine the time delays. In particular, this concerns neurophysiological time delays determined by factors such as signal propagation velocities and distances between cortical sites, muscles, and receptors, as well as time delays associated with signal transmission times in man-machine interactions and human interactions (visual, acoustic, haptic).

Third, due to the sensitivity of the performance variability on time delays, it might be the case that the functionality of motor control systems breaks down when time delays are changed by relatively little amounts. In this context, not only the sensitivity of the variability plays an important role, but also the fact that mean energy and degree of disorder (as measured in terms of entropy) crucially depend on the time delay. Changing a time delay by a few percent may result in a change of the mean energy and the degree of disorder by 100 or more percent. All kinds of amplification factors are possible.

Fourth, the overshoot phenomenon as well as the destabilization resonances suggest—counterintuitively—that it might be useful for motor control systems to increase time delays. The reason for this is that due to structural constraints of the human body, time delays cannot be decreased beyond certain thresholds. Signals need to travel certain distances (e.g., from a cortical site in the head to the toe of a foot) and signals can only travel with particular maximum speeds. If a motor control system somehow involves a particular time

delay such that the system operates at the falling edge of a resonance peak or an overshoot hillock, then it might be impossible to decrease the time delay by a sufficiently large amount such that the variances σ_p^2 and σ_x^2 become smaller as the system has been pushed over the resonance peak or the overshoot hillock. In such situations, the only option that we have to improve performance and to decrease performance variability is to increase the time delay.

Finally, we would like to point out that these considerations also shed new light on the wiring of neural pathways. Since the pathway lengths of a neural network determine (among other factors) the time delays to which the network is subjected, the pathway lengths may play a crucial role for the functioning of a neural network.

VI. CONCLUSIONS

In the present paper, we studied the stochastic properties of dynamical systems subjected to fluctuating forces and time-delayed feedback loops that can be described in terms of linear stochastic delay differential equations of second order. We assumed that the systems can be described in terms of (generalized) position and momentum variables (x and p) such that the second-order evolution equations can be regarded as Kramers equations with time delay. For this class of systems, we showed that the stationary distributions are Gaussian distributions and derived analytical expressions for the variances σ_p^2 and σ_x^2 of the momentum and position variables. Furthermore, we identified two qualitatively different parameter regimes by means of the parameters a and b related to a nondelayed and a time-delayed friction force. In the first parameter regime given by $b<a$, stationary distributions exist for all time delays. In the second parameter regime given by $b \geqslant a$, a more detailed discussion is necessary. For $b \geqslant a$, we showed that there is set of critical time delays $\tau_{u,j}$ and $\tau_{s,j}$ at which the first moments of x and p become unstable and become stable again by means of Hopf bifurcations. We showed explicitly that at these Hopf bifurcation points the variances σ_p^2 and σ_x^2 become infinite (for $\tau_{u,j}$) to then become finite again (for $\tau_{s,j}$).

In particular, for $b>a$, stationary distributions with finite variances exist for delays τ with $0 \leqslant \tau < \tau_{u,0}$ and $\tau_{s,j} < \tau < \tau_{u,j+1}$. Otherwise, they do not exist. That is, we derived a stochastic description of time-delayed systems that can exhibit re-entrant bifurcations. In line with earlier works on double Hopf bifurcations [52,53], we argued that the sequence of re-entrant bifurcations is truncated because the characteristic equations of the corresponding deterministic systems exhibit imaginary solutions $\lambda = \pm i\omega$ with multiplicity two (double Hopf bifurcation points). We demonstrated that the parameter domains in which stationary distributions exist can be conveniently determined by means of stability diagrams in the a-τ plane that reveal some kind of Christmas tree structure. For $b=a$, we found that the variances σ_p^2 and σ_x^2 exhibit an infinite set of singularity points which are related to the (right hand side) boundary points of the aforementioned Christmas tree stability graphs. For $b=a$, the critical delays $\tau_{u,j}$ and $\tau_{s,j}$ merge and correspond in the stability graphs to a set of right hand side boundary points. As a result, we found that stationary distributions with finite variances exist for all delays except for delays that correspond to these boundary points.

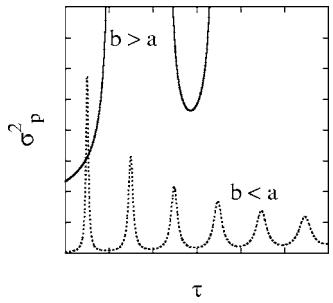

FIG. 13. Qualitative functional dependencies of variances σ_p^2 on time delays τ for second-order dynamical models of the form (2) and (3) [solid line: $b>a$; dashed line: $b<a$ with $b^2 > a^2 - (4k/m)$].

Close to the critical line $b=a$ in the parameter space (a,b) (i.e., for $b=a-\epsilon$ with $\epsilon>0$ small), the variances σ_p^2 and σ_x^2 oscillate as functions of the time delays and exhibit pronounced peaks at regular intervals. These oscillations can be interpreted in terms of destabilization resonances related to the oscillatory instabilities that exist in the adjacent parameter regime (i.e., for $b \geqslant a$). In short, we observed time-delayed destabilization resonances due to oscillatory ghost instabilities. Similar resonances have recently been found for the correlation time of trajectories produced by time-delayed van der Pol oscillators [50]. We may speculate that the correlation time resonances reported in Ref. [50] are related to the aforementioned ghost instabilities as well.

Finally, we have shown that the variances σ_p^2 and σ_x^2 can feature overshoots. That is, the variances exhibit maxima at particular time delays $\tau_{\max}$. These maxima separate the functions $\sigma_p^2(\tau)$ and $\sigma_x^2(\tau)$ into rising and falling functions for delays $\tau < \tau_{\max}$ and $\tau > \tau_{\max}$, respectively.

We would like to underscore that the aforementioned re-entrant bifurcations, destabilization resonances and overshoots are phenomena that arise due to a dimensionality effect. In the one-dimensional time-delayed systems (i.e., systems described by linear first-order stochastic delay differential equations) these phenomena cannot be observed. Re-entrant bifurcations, destabilization resonances, and overshoots can be observed if we add a degree of freedom to the one-dimensional systems, that is, if we consider two-dimensional time-delayed systems. For one-dimensional time-delayed systems, Fig. 1 summarizes the possible qualitative dependencies of variances on time delays. For the corresponding two-dimensional systems, Fig. 13 depicts the possible functional dependencies. When the two-dimensional systems are reduced to one-dimensional ones (which happens in our case in the limit $k \to 0$), Fig. 13 will be distorted to recover Fig. 1. Alternatively, we may say that these novel phenomena arise due to the impact of the harmonic restoring force $F(x) = -kx$.

We discussed implications of our theoretical results for human motor control systems. We reinterpreted previous experimental studies on time-delayed tracking movements and showed that experimental findings obtained earlier suggest that the second-order dynamical model has physical rel-

evance for both the parameter domain $b>a$ and $a>b$. In addition, we made some predictions based on our second-order dynamical model concerning the stochastic behavior of human motor control systems. Accordingly, it seems plausible that destabilization resonances, delay-induced minima of performance variability as depicted in Fig. 13, and overshoots could be observed in human motor performance. In particular, we have emphasized that the rule of thumb, which states that time delays destabilize systems, does not hold in general for time-delayed second-order dynamical systems, see Fig.13 . We would like to point out that our reinterpretations as well as our predictions have to be verified by future experimental studies because so far experiments have not been carried out to test specific predictions from the Kramers model involving time delays.

At this juncture, it is useful to return also to the issue of multiplicative versus additive noise. The question arises to what extent the results derived in Secs. II–V carry over if we are dealing with motor control systems dominated by multiplicative noise. Previous theoretical studies on first-order dynamical systems involving time delays and multiplicative noise [42,45] revealed that multiplicative and additive noise systems have in common that we can determine (at least by semianalytical methods) the parameter domains in which stationary distributions exist. These studies, however, also revealed that the derivation of autocorrelation functions and variances becomes mathematically involved and in general leads to a set of time-delayed moment equations that is not closed. It is reasonable to assume that in the case of second-order dynamical systems with time delays and multiplicative noise, a similar situation will be encountered. Most likely these systems will reveal qualitatively the same behavior in particular parameter domains as their additive noise counterparts. That is, re-entrant bifurcations as depicted in Fig. 13, destabilization resonances, and overshoots are likely to occur. Given the current technical difficulties in the analysis of time-delayed systems with multiplicative noise, two promising alternative approaches are the study of reducible systems and the utilization of perturbation theoretical methods. In the first case, multiplicative noise systems are mapped to additive noise systems by means of variable transformations. For systems without time delays, this procedure belongs nowadays to the standard literature [60] and has only recently been generalized to systems involving time delays [44,49,76]. In the second case, analytical results may be derived for multiplicative noise systems that involve small time delays or small coupling parameters that describe the impact of weakly interfering time-delayed feedback loops [43,67,77].

This work was financially supported by the Thailand Research Fund, Contract No. PHD/0241/2545.3.M.MU/45/B.1.

APPENDIX A: DERIVATION OF EQ. (30)

To begin with, we note that Eq. (29) can be written as

$$Z^{(1)}(\tau) = \frac{\theta_1 - \theta_2}{a + b\cos(\omega_2\tau)}, \tag{A1}$$

where

$$\theta_i = [a + b\cos(\omega_j\tau)][\omega_i b\sin(\omega_i\tau) - \omega_i^2 + (k/m)]. \tag{A2}$$

Consequently, Eq. (26) becomes

$$C_1^{(1)}(\tau) = \frac{f(\tau)}{\theta_1 - \theta_2}, \tag{A3}$$

where

$$f(\tau) = \frac{Q}{2}\left\{\left(a - b\frac{\omega_1^2\cos(\omega_1\tau) - \omega_2^2\cos(\omega_2\tau)}{\omega_1^2 - \omega_2^2}\right)(a + b\cos(\omega_2\tau)) - bB^{(1)}(\tau)(b\omega_2\sin(\omega_2\tau) - \omega_2^2 + (k/m))\right\}. \tag{A4}$$

Using Eq. (24) in terms of

$$\omega_i\sqrt{b^2 - a^2} = \omega_i^2 - \frac{k}{m}, \tag{A5}$$

the first term of $f(\tau)$ becomes

$$\frac{1}{\omega_1^2\omega_2^2}\{\omega_1^2[a - b\cos(\omega_1\tau)][a + b\cos(\omega_2\tau)] - \omega_2^2[a^2 - b^2\cos^2(\omega_2\tau)]\}. \tag{A6}$$

The second term of $f(\tau)$ becomes

$$\frac{1}{\omega_1^2 - \omega_2^2}\{\omega_2^2(b^2\sin^2(\omega_2\tau) - (b^2 - a^2)) - \omega_1\omega_2(b\sin(\omega_1\tau) + \sqrt{b^2 - a^2})(b\sin(\omega_2\tau) - \sqrt{b^2 - a^2})\}. \tag{A7}$$

With the help of the trigonometric relation

$$a^2 - b^2\cos^2(\omega_i\tau) = b^2\sin^2(\omega_i\tau) - (b^2 - a^2), \tag{A8}$$

we obtain

$$f(\tau) = \frac{Q}{2(\omega_1^2 - \omega_2^2)}\{\omega_1^2(a - b\cos(\omega_1\tau))(a + b\cos(\omega_2\tau)) - \omega_1\omega_2(b\sin(\omega_1\tau) + \sqrt{b^2 - a^2})(b\sin(\omega_2\tau) - \sqrt{b^2 - a^2})\}. \tag{A9}$$

Using

$$a - b\cos(\omega_1\tau) = \frac{a^2 - b^2\cos^2(\omega_1\tau)}{a + b\cos(\omega_1\tau)} \tag{A10}$$

and Eq. (A8), we then have

$$f(\tau) = \frac{Q}{2(\omega_1^2 - \omega_2^2)}\left\{\frac{b\sin(\omega_1\tau) + \sqrt{b^2 - a^2}}{a + b\cos(\omega_1\tau)}\right\}\{\theta_1 - \theta_2\}. \tag{A11}$$

From Eqs. (A3) and (A11), we conclude that Eq. (30) holds.

APPENDIX B: DERIVATION OF EQ. (43)

For the underdamped case, that is, for $b<a$ and $b^2>a^2 - (4k/m)$, we use the autocorrelation function

$$C^{(2)}(z) = C_1^{(2)} \cosh(\omega_1 z) + e_1^{(2)} \sinh(\omega_1 z) + C_2^{(2)} \cosh(\omega_2 z) + e_2^{(2)} \sinh(\omega_2 z), \tag{B1}$$

where $\omega_{1,2}=u\pm vi$ are complex values with $v\neq 0$. Consequently, we obtain for $C_1^{(2)}$, $C_2^{(2)}$, $e_1^{(2)}$, and $e_2^{(2)}$ the same formal expressions as for $C_1^{(3)}$, $C_2^{(3)}$, $e_1^{(3)}$, and $e_2^{(3)}$. The hyperbolic functions in Eq. (B1) read like

$$\begin{aligned}
\cosh(\omega_1\tau) &= \cosh(u\tau)\cos(v\tau) + i\sinh(u\tau)\sin(v\tau),\\
\cosh(\omega_2\tau) &= \cosh(u\tau)\cos(v\tau) - i\sinh(u\tau)\sin(v\tau),\\
\sinh(\omega_1\tau) &= \sinh(u\tau)\cos(v\tau) + i\cosh(u\tau)\sin(v\tau),\\
\sinh(\omega_2\tau) &= \sinh(u\tau)\cos(v\tau) - i\cosh(u\tau)\sin(v\tau),
\end{aligned} \tag{B2}$$

and we see that $\omega_1=\omega_2^*$, $\cosh(\omega_1\tau)=[\cosh(\omega_2\tau)]^*$ and $\sinh(\omega_1\tau)=[\sinh(\omega_2\tau)]^*$, where the star denotes the complex conjugate. Applying these relations to the parameters $e_1^{(2)}=e_1^{(3)}$ and $e_2^{(2)}=e_2^{(3)}$ defined in Sec. II B, we find $e_1^{(2)}=[e_2^{(2)}]^*$. Since $C(z)$ is a real-valued function, it is clear from Eq. (B1) that $C_1^{(2)}=[C_2^{(2)}]^*$. Consequently, the variance of p can be written as

$$\sigma_p^{2(2)} = C^{(2)}(0) = 2\,\mathrm{Re}\{C_1^{(2)}\}. \tag{B3}$$

We put $C_1^{(2)}=C_1^{(3)}$, where $C_1^{(3)}$ is given by Eqs. (36)–(38). Next, we substitute the relations (B2) into Eqs. (36)–(38). Thus, we obtain the complex-valued parameter $C_1^{(2)}$. Taking the real part and multiplying with the factor 2, we obtain Eq. (43), where

$$\begin{aligned}
A_1 &= [a + b\cosh(u\tau)\cos(v\tau)]\{2uv - b[v\sinh(u\tau)\cos(v\tau) + u\cosh(u\tau)\sin(v\tau)]\} - b\sinh(u\tau)\sin(v\tau)\{2u^2 + b[v\cosh(u\tau)\sin(v\tau) - u\sinh(u\tau)\cos(v\tau)]\},\\
A_2 &= -2uv + b[v\sinh(u\tau)\cos(v\tau) + u\cosh(u\tau)\sin(v\tau)],\\
A_3 &= 2uv + b[v\sinh(u\tau)\cos(v\tau) + u\cosh(u\tau)\sin(v\tau)],\\
A_4 &= 2uv[a - b\cosh(u\tau)\cos(v\tau)] - b(u^2 - v^2)\sinh(u\tau)\sin(v\tau).
\end{aligned} \tag{B4}$$

APPENDIX C: SPECIAL CASES

1. Case $a=b>0$

In order to discuss the case $a=b$, we exploit the results previously derived in Sec. II B. That is, we consider the limiting case $b\to a^+$ for $b>a$. We write the variance of p given by Eq. (31) in the form

$$\sigma_p^{2(1)}(\tau) = \frac{bQB^{(1)}(\tau)}{2[a + b\cos(\omega_2\tau)]}\left\{B^{(1)}(\tau) + \xi(\tau)\frac{[\cos(\omega_2\tau) - \cos(\omega_1\tau)]}{Z^{(1)}(\tau)}\right\}, \tag{C1}$$

where $\xi(\tau)$ is defined by

$$\xi(\tau) = a - b\frac{\omega_1^2\cos(\omega_1\tau) - \omega_2^2\cos(\omega_2\tau)}{\omega_1^2 - \omega_2^2} - bB^{(1)}(\tau)\frac{b\omega_2\sin(\omega_2\tau) - \omega_2^2 + (k/m)}{a + b\cos(\omega_2\tau)}. \tag{C2}$$

From Eq. (24), it can be seen that

$$\omega_1 = \sqrt{\frac{k}{m}} = \omega_0, \qquad \omega_2 = -\sqrt{\frac{k}{m}} = -\omega_0 \tag{C3}$$

in the limit $b\to a^+$. In addition, we find

$$\lim_{b\to a^+} B^{(1)}(\tau) = \frac{2\omega_0 + a\tau\omega_0\cos(\omega_0\tau) + a\sin(\omega_0\tau)}{2\omega_0 a}, \tag{C4}$$

$$\lim_{b\to a^+} Z^{(1)}(\tau) = 0, \tag{C5}$$

and

$$\lim_{b\to a^+} \xi(\tau) = \frac{\sin(\omega_0\tau)}{2[1 + \cos(\omega_0\tau)]}[a\sin(\omega_0\tau) + a\omega_0\tau - 2\omega_0]. \tag{C6}$$

Furthermore, the most right standing term in Eq. (C1) yields

$$\lim_{b\to a^+} \frac{[\cos(\omega_2\tau) - \cos(\omega_1\tau)]}{Z^{(1)}(\tau)} = \frac{\tau\sin(\omega_0\tau)}{\tau a\omega_0 - 2\omega_0 + a\sin(\omega_0\tau)}. \tag{C7}$$

Using Eqs. (C4), (C6), and (C7), we obtain

$$\lim_{b\to a^+} \sigma_p^{2(1)}(\tau) = \frac{Q}{4[1 + \cos(\omega_0\tau)]} \times \left\{\frac{2\omega_0 + a\tau\omega_0\cos(\omega_0\tau) + a\sin(\omega_0\tau)}{\omega_0 a} + \tau[1 - \cos(\omega_0\tau)]\right\}. \tag{C8}$$

Consequently, we have

$$\lim_{b\to a^+} \sigma_x^{2(1)}(\tau) = \frac{1}{km\omega_0}\left\{\lim_{b\to a^+} \sigma_p^2(\tau)[\omega_0 - a\sin(\omega_0\tau)] + \frac{Q}{4}\tau a\sin(\omega_0\tau)\right\}. \tag{C9}$$

2. Case $k=0$

Finally, the variances obtained in previous studies on systems with overdamped first-order dynamics [40,41] will be compared with the variances derived from the Kramers equations (2) and (3) in the special case $k=0$. For $k=0$, Eq. (3) becomes the first-order stochastic delay differential equation

(5). In Refs. [40,41], it has been shown that the stationary probability density of p is given by Eq. (6), and that the variance of p has the form

$$\sigma_p^2 = \begin{cases} \frac{Q}{2}\left(\frac{1+b\omega^{-1}\sin(\omega\tau)}{a+b\cos(\omega\tau)}\right), & b>a\geqslant 0 \\ \frac{Q}{2}\left(\frac{1+b\omega^{-1}\sinh(\omega\tau)}{a+b\cosh(\omega\tau)}\right), & a>b\geqslant 0 \\ \frac{Q}{4a}(1+a\tau), & a=b>0 \end{cases} \quad \text{(C10)}$$

where $\omega=\sqrt{|a^2-b^2|}$. Now, let us derive Eq. (C10) from the results presented in Sec. II B. First, we consider the case $b>a\geqslant 0$ and $k=0$. From Eq. (24), we have $\omega_1=\sqrt{b^2-a^2}=\omega$ and $\omega_2=0$. Consequently, $C_1^{(1)}$ given by Eq. (30) becomes

$$C_1^{(1)} = \frac{Q}{2}\left(\frac{1+b\omega^{-1}\sin(\omega\tau)}{a+b\cos(\omega\tau)}\right). \quad \text{(C11)}$$

From Eq. (28) it is clear that $B^{(1)}(\tau)=b^{-1}[1+\omega/b\sin(\omega\tau)]$. As a result, Eq. (27) reduces to

$$C_2^{(1)}(\tau) = \frac{Q/2[1+\omega/b\sin(\omega\tau)]-[a+b\cos(\omega\tau)]C_1^{(1)}(\tau)}{a+b}. \quad \text{(C12)}$$

Using Eq. (C11), we see that $C_2^{(1)}(\tau)=0$. From Eq. (31), it then follows that

$$\sigma_p^{2(1)}(\tau) = C_1^{(1)}(\tau) = \frac{Q}{2}\left(\frac{1+b\omega^{-1}\sin(\omega\tau)}{a+b\cos(\omega\tau)}\right). \quad \text{(C13)}$$

Similarly, for the overdamped case $[b<a,\ b^2<a^2-(4k/m)]$ it is easy to verify that for $k\to 0$, the variance (41) reduces to

$$\sigma_p^{2(3)} = \frac{Q}{2}\left(\frac{1+b\omega_1^{-1}\sinh(\omega_1\tau)}{a+b\cosh(\omega_1\tau)}\right), \quad \text{(C14)}$$

with $\omega_1=\sqrt{a^2-b^2}=\omega$. Finally, we consider the case $a=b>0$. If $k=0$, then from Eq. (C3) we have $\omega_0=0$. Substituting $\omega_0=0$ into Eq. (C8), we obtain

$$\lim_{b\to a^+}\sigma_p^{2(1)}(\tau) = \frac{Q}{4a}(1+a\tau). \quad \text{(C15)}$$

[1] R. Lang and K. Kobayashi, IEEE J. Quantum Electron. **16**, 347 (1980).
[2] K. Ikeda and O. Akimoto, Phys. Rev. Lett. **48**, 617 (1982).
[3] T. Erneux, L. Lager, M. W. Lee, and J. Goedgebuer, Physica D **194**, 49 (2004).
[4] L. Larger, J. P. Goedgebuer, and T. Erneux, Phys. Rev. E **69**, 036210 (2004).
[5] N. Khrustova, G. Veser, A. Mikhailov, and R. Imbihl, Phys. Rev. Lett. **75**, 3564 (1995).
[6] E. Villermaux, Phys. Rev. Lett. **75**, 4618 (1995).
[7] L. S. Tsimring and A. Pikovsky, Phys. Rev. Lett. **87**, 250602 (2001).
[8] C. Masoller, Phys. Rev. Lett. **90**, 020601 (2003).
[9] K. Pyragas, Phys. Lett. A **170**, 421 (1992).
[10] N. S. Goel, S. C. Maitra, and E. W. Montroll, Rev. Mod. Phys. **43**, 231 (1971).
[11] J. M. Cushing, *Integrodifferential Equations and Delay Models in Population Dynamics* (Springer, Berlin, 1977).
[12] C. T. H. Baker, G. Bocharov, C. A. H. Paul, and F. A. Rihan, J. Math. Biol. **37**, 341 (1998).
[13] M. C. Mackey and L. Glass, Science **197**, 287 (1977).
[14] T. D. Frank and P. J. Beek, Phys. Rev. E **64**, 021917 (2001).
[15] P. Tass, J. Kurths, M. G. Rosenblum, G. Guasti, and H. Hefter, Phys. Rev. E **54**, R2224 (1996).
[16] U. Langenberg, H. Hefter, K. R. Kessler, and J. D. Crooke, Exp. Brain Res. **118**, 161 (1998).
[17] F. Ishida and Y. E. Sawada, Phys. Rev. Lett. **93**, 168105 (2004).
[18] K. U. Smith, *Delayed Sensory Feedback and Behavior* (W. B. Saunders Company, Philadelphia, 1962).
[19] G. Stepan, *Retarded Dynamical Systems: Stability and Characteristic Functions* (Longman Scientific & Technical, New York, 1989).
[20] J. L. Cabrera and J. G. Milton, Phys. Rev. Lett. **89**, 158702 (2002).
[21] J. Sieber and B. Krauskopf, Physica D **197**, 332 (2004).
[22] C. W. Eurich and J. G. Milton, Phys. Rev. E **54**, 6681 (1996).
[23] T. Ohira and J. G. Milton, Phys. Rev. E **52**, 3277 (1995).
[24] R. J. Peterka, Biol. Cybern. **82**, 335 (2000).
[25] K. Vasilakov and A. Beuter, J. Theor. Biol. **165**, 389 (1993).
[26] T. D. Frank, P. J. Beek, and R. Friedrich, Phys. Lett. A **338**, 74 (2005).
[27] Y. Chen, M. Ding, and J. A. Scott Kelso, Phys. Rev. Lett. **79**, 4501 (1997).
[28] H. Hasegawa, Phys. Rev. E **70**, 021912 (2004).
[29] H. Haken, *Brain Dynamics* (Springer, Berlin, 2002).
[30] A. Hutt, Phys. Rev. E **70**, 052902 (2004).
[31] M. G. Rosenblum and A. S. Pikovsky, Phys. Rev. Lett. **92**, 114102 (2004).
[32] H. Sompolinsky, D. Golomb, and D. Kleinfeld, Phys. Rev. A **43**, 6990 (1991).
[33] V. K. Jirsa and M. Ding, Phys. Rev. Lett. **93**, 070602 (2004).
[34] G. A. Bocharov and F. A. Rihan, J. Comput. Appl. Math. **125**, 183 (2000).
[35] R. R. Neptune and S. A. Kautz, Exercise Sport Sci. Rev. **29**, 76 (2001).
[36] G. J. Lehman, D. Lennon, B. Tresidder, B. Rayfield, and M. Poschar, Musculoskeletal Dis. **5**, 3 (2004).
[37] J. Hale, *Theory of Functional Differential Equations* (Springer, Berlin, 1977).
[38] R. D. Driver, *Ordinary and Delay Differential Equations—Applied Mathematical Sciences* (Springer, New York, 1977), Vol. 20.
[39] M. Schanz and A. Pelster, Phys. Rev. E **67**, 056205 (2003).
[40] T. D. Frank, P. J. Beek, and R. Friedrich, Phys. Rev. E **68**, 021912 (2003).

[41] U. Küchler and B. Mensch, Stoch. Stoch. Rep. **40**, 23 (1992).
[42] M. C. Mackey and I. G. Nechaeva, Phys. Rev. E **52**, 3366 (1995).
[43] S. Guillouzic, I. L' Heureux, and A. Longtin, Phys. Rev. E **59**, 3970 (1999).
[44] A. A. Budini and M. O. Caceres, Phys. Rev. E **70**, 046104 (2004).
[45] T. D. Frank, Phys. Rev. E **69**, 061104 (2004).
[46] S. Guillouzic, I. L' Heureux, and A. Longtin, Phys. Rev. E **61**, 4906 (2000).
[47] A. A. Gushchin and U. Küchler, Rev. Union Mat. Argent. Asoc. Fis. Argent. **88**, 195 (2000).
[48] E. I. Verreist, in *Advances in Time-Delay Systems*, edited by S. I. Niculescu and K. Gu (Springer, Berlin, 2004), pp. 390–420.
[49] T. D. Frank, K. Patanarapeelert, and I. M. Tang, Phys. Lett. A **339**, 246 (2005).
[50] N. B. Janson, A. G. Balanov, and E. Schöll, Phys. Rev. Lett. **93**, 010601 (2004).
[51] O. V. Popovych, C. Hauptmann, and P. A. Tass, Phys. Rev. Lett. **94**, 164102 (2005).
[52] S. A. Campbell, J. Bélair, T. Ohira, and J. Milton, J. Dyn. Differ. Equ. **7**, 213 (1995).
[53] S. A. Campbell, J. Bélair, T. Ohira, and J. Milton, Chaos **5**(4), 640 (1995).
[54] U. an der Heiden, A. Longtin, M. Mackey, J. Milton, and R. Scholl, J. Dyn. Differ. Equ. **2**, 423 (1990).
[55] W. Bayer and U. an der Heiden, J. Dyn. Differ. Equ. **10**, 303 (1998).
[56] U. an der Heiden and W. Bayer, Nonlinear Anal.: Real World Appl. **48**, 461 (2002).
[57] R. Sipahi and N. Olgac, in *Advances in Time-Delay Systems*, edited by S. I. Niculescu and K. Gu (Springer, Berlin, 2004), pp. 61–73.
[58] J. A. Anderson and M. W. Sponge, IEEE Trans. Autom. Control **34**, 494 (1989).
[59] H. Haken, *Synergetics: Introduction and Advanced Topics* (Springer, Berlin, 2004).
[60] W. Horsthemke and R. Lefever, *Noise-Induced Transitions* (Springer, Berlin, 1984).
[61] A. Longtin, J. G. Milton, J. E. Bos, and M. C. Mackey, Phys. Rev. A **41**, 6992 (1990).
[62] L. Stark, F. W. Campbell, and J. Atwood, Nature (London) **182**, 857 (1958).
[63] S. Usui and L. Stark, Biol. Cybern. **45**, 13 (1982).
[64] C. M. Harris and D. M. Wolpert, Nature (London) **394**, 780 (1998).
[65] P. B. Matthews, J. Physiol. (London) **492**, 597 (1996).
[66] H. Risken, *The Fokker-Planck Equation—Methods of Solution and Applications* (Springer, Berlin, 1989).
[67] T. D. Frank, Phys. Rev. E **71**, 031106 (2005).
[68] S. A. Campbell, Dynamics of Continuous, Discrete and Impulsive Systems **5**, 225 (1999).
[69] K. L. Cooke and Z. Grossman, J. Math. Anal. Appl. **86**, 592 (1982).
[70] S. A. Campbell and J. Bélair, Canad. Appl. Math. Quart. **7**, 218 (1999).
[71] F. G. Boese, J. Math. Anal. Appl. **140**, 510 (1989).
[72] J. A. S. Kelso, *Dynamic Patterns—The Self-Organization of Brain and Behavior* (MIT Press, Cambridge, 1995).
[73] H. Haken, *Principles of Brain Functioning* (Springer, Berlin, 1996).
[74] P. G. Amazeen, E. Amazeen, and M. T. Turvey, in *Timing of Behavior*, edited by D. A. Rosenbaum and C. E. Collyer (MIT Press, Cambridge, 1998), pp. 237–259.
[75] A. A. Post, C. E. Peper, A. Daffertshofer, and P. J. Beek, Biol. Cybern. **83**, 443 (2000).
[76] K. Patanarapeelert, T. D. Frank, R. Friedrich, and I. M. Tang, J. Phys. A **38**, 10069 (2005).
[77] T. D. Frank, Phys. Rev. E **72**, 011112 (2005).
[78] Note that although we have assigned now to all parameters and variables particular meanings and units (e.g., x is the position or elongation of an oscillator that might be measured in meters), Eqs. (2) and (3) may be applied in different contexts (e.g., error dynamics), which will require reinterpretations of all parameters and variables and their units. To stress this generality of our model, we will simply regard all parameters and variables as dimensionless entities.
[79] Note that one can prove rigorously that σ_p^2 increases monotonically. To this end, first note that $C_1^{(1)}(\tau)$ given by Eq. (30) is a monotonically increasing function for $[0,\tau_{u,0})$ as shown in a previous study [45]. Note further that $\omega_1>0$ and $\omega_2<0$ which implies that $B^{(1)}(\tau)$, $-[a+b\cos(\omega_1\tau)]$, and $1/[a+b\cos(\omega_2\tau)]$ are monotonically increasing functions for $[0,\tau_{u,0})$. From Eq. (27) it then follows that $C_2^{(1)}(\tau)$ is a monotonically increasing function. Therefore, $\sigma_p^2(\tau)=C_1^{(1)}(\tau)+C_2^{(1)}(\tau)$ increases monotonically with τ in the domain $[0,\tau_{u,0})$.
[80] The notion of ghost instabilities is the counterpart of the notion of ghost attractors used in the theory of dynamical systems.